Forest Service
U.S. DEPARTMENT OF AGRICULTURE

Forest Products Laboratory | General Technical Report FPL–GTR–294 | November 2022

Review of Industrial-Grade Cellulosic Nanomaterial Composites

Gregory T. Schueneman
Robert J. Moon

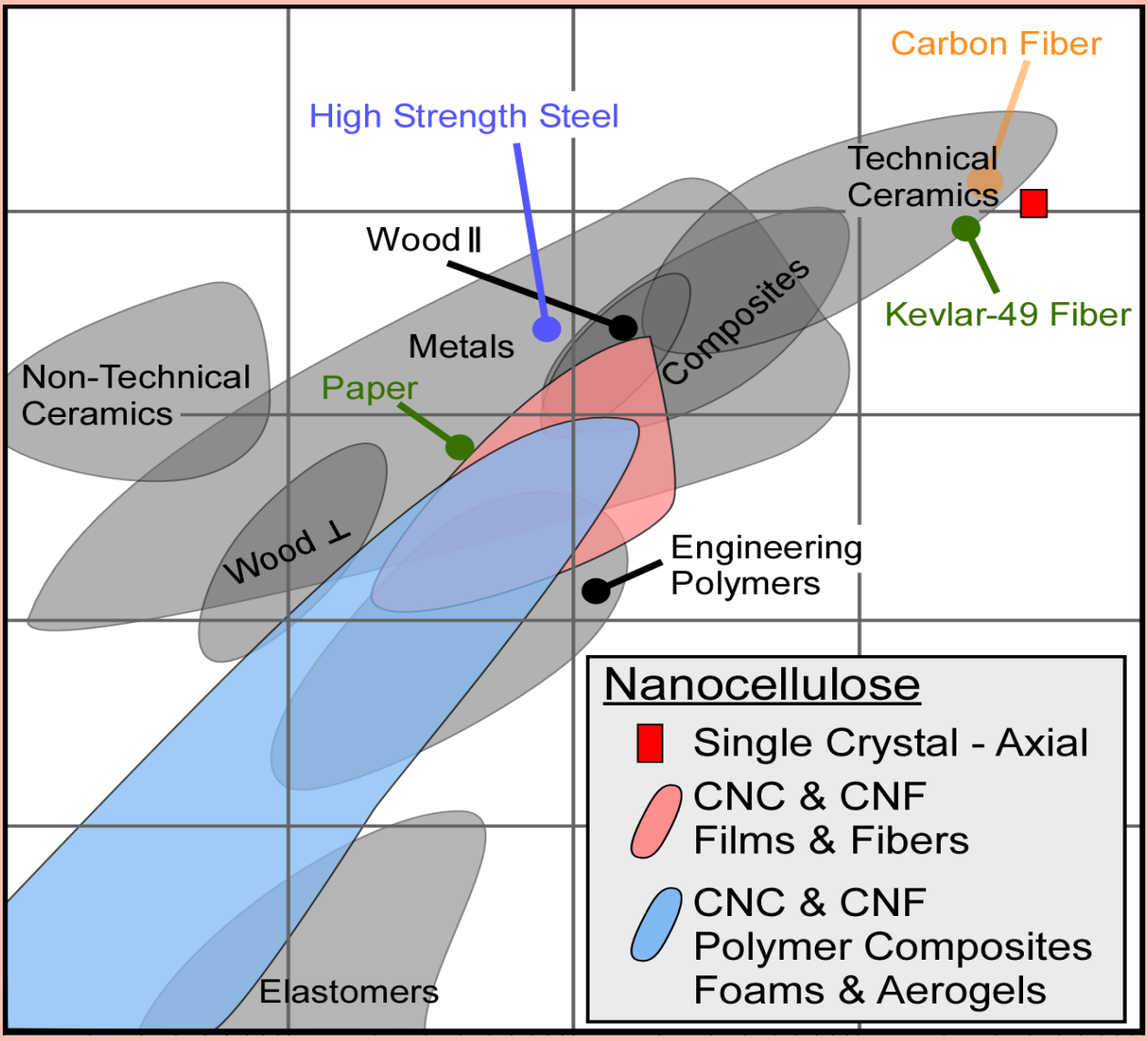

Abstract

Cellulose nanomaterials derived from wood, plants, and other organisms provide mechanical reinforcement to a wide variety of polymers. The reproducibility and uniformity of these bioderived and biodegradable nanomaterials makes them suitable for use in existing petrochemical-derived polymers and resins in which relatively simple and pure molecules are used. The composites benefit from improved mechanical, thermal, rheological, and other properties while imparting biobased content (new carbon), thereby sequestering carbon in a multitude of products. The refractive index match between cellulose and polymers results in generally maintained transparency such that the appearance of the final product is not altered. In this report, we critically review the cellulosic nanomaterial–polymer composite literature and seek out those materials and methods that are most suitable for industrial adoption based on ease of use and performance improvements. This review covers promising composite fabrication approaches with waterborne and freeze-dried cellulose nanomaterials and other methods that uniquely prepare composites or prepare surfaces for ease of dispersion. In addition, knowledge gaps and research needs are summarized.

Keywords: critical review; industrial adoption; cellulosic nanomaterials; composites; waterborne; freeze-dried

Contents

November 2022

Schueneman, G.T.; Moon, R.J. 2022. Review of industrial-grade cellulosic nanomaterial composites. General Technical Report FPL-GTR-294. Madison, WI: U.S. Department of Agriculture, Forest Service, Forest Products Laboratory. 21 p. https://doi.org/10.2737/FPL-GTR-294.

USDA Forest Service, Forest Products Laboratory
One Gifford Pinchot Drive, Madison, WI, USA 53726
(608) 231-9200
SM.FS.MailroomFPL@usda.gov

This and many other Forest Service research publications are available for download through TreeSearch at https://www.fs.usda.gov/treesearch/.

The Forest Products Laboratory is maintained in cooperation with the University of Wisconsin.

Review of Industrial-Grade Cellulosic Nanomaterial Composites

Gregory T. Schueneman, Materials Research Engineer
Robert J. Moon, Materials Research Engineer
USDA Forest Service, Forest Product Laboratory, Madison, WI, USA

1. Introduction

Cellulose is ubiquitous in the world, and the benefit from it and the progress humankind has achieved with it are immeasurable. The extraction of nanomaterials from cellulose is of relatively recent interest even though this discovery is more than a century old (Herzog and Jancke 1920) with the first electron micrographs published in the 1950s (Ranby 1949, 1951, 1952; Ranby and Ribi 1950). It is the realization that nanomaterials offer great benefits to materials science and many other fields that has focused intensive research on the evaluation and utilization of cellulosic nanomaterials (CNs). The past two decades have seen a rapidly growing base of research teams with increasing numbers of publications and patents, and this has significantly accelerated in the past 5 years. Many discoveries have been achieved in the areas of polymer composites, paper, packaging, adhesives, inks, hygiene, etc. (Moon and others 2016). However, despite the realized benefit of CN additions to polymer composites, industrial utilization is lacking. Why? What is holding industry back from picking up this technology and incorporating it into product lines that serve increasingly environmentally conscious or concerned consumers? This review investigates this question.

There are numerous review articles that provide detailed descriptions of the extraction and characteristics of CNs in their various forms. Thus, this review will not cover introductory or background information, and the reader is directed to the numerous review articles that cover this topic (Foster and others 2018, Habibi 2014, Habibi and others 2010, Moon and others 2011). It is important to note that there are many varieties of CNs, presenting a wide spectrum of particle morphologies (e.g., shape, size, and aspect ratio), properties, and surface chemistries, all of which affect the processing and performance of CN additions to polymer composites. A comprehensive understanding of which still remains elusive. In this review, the terminology used to define cellulose nanocrystals (CNCs), cellulose nanofibrils (CNFs), and cellulose microfibrils (CMFs) conforms to Canadian standard CSA Z5100-14 (CSA Group 2014). Figure 1 shows the differences in the CN particle morphology. CNCs are more rod-like, whereas CNFs are more fibril-like. An important background clarification is that CNs extracted with sulfuric acid, phosphoric acid, or TEMPO (2,2,6,6-tetramethylpiperidinyloxy) are hydrophilic and ionic. This circumstance makes their handling fundamentally different from extraction methods that yield purely hydroxylated surfaces such as hydrochloric acid. The ionic character of the CNs generates a self-dispersing character in water, whereas a native cellulose surface is not water dispersible for long periods of time. However, this advantage, which aids in the extraction and handling, poses a challenge when seeking to convert ionic-containing surfaces to be compatible with hydrophobic polymers or resins. Thus, the success or failure of a composite approach is dictated by how it addresses this and other issues.

This review critically assessed CN literature to seek out and identify approaches that successfully incorporated CNs into hydrophobic polymer–resin matrixes via industrially viable methods for significant performance enhancements. With industry relevancy in mind, this review excluded approaches that used complex or time-consuming steps, solvent casting, toxic or difficult to work with solvents, or high gravitational/speed centrifugation as they are deemed not generally industrially viable. Also excluded were those approaches that resulted in insignificant improvements in mechanical performance. Often, the reported mechanical performance improvement is statistically significant; however, CNs may not be industrially significant as a performance additive, especially compared with the existing additive alternatives that provide equal or greater performance enhancements. Generally speaking, the performance enhancement must clearly exceed the combined variance or standard deviations in the results and in addition be greater than a 20% to 30% improvement compared with the unreinforced matrix. Beyond these relatively stringent exclusions, several additional polymer–resin matrixes were excluded because of their low degree of focus in literature or for being hydrophilic, as in the case of poly(vinyl alcohol). These are not typically matrixes for the hydrophobic polymers used in industry. The benefit of this narrowed focus is that it gives an opportunity to conduct an exhaustive critical exploration and reporting of factors influencing mechanical performance of CNs to industry relevant polymer–resin systems. Nonetheless, it is

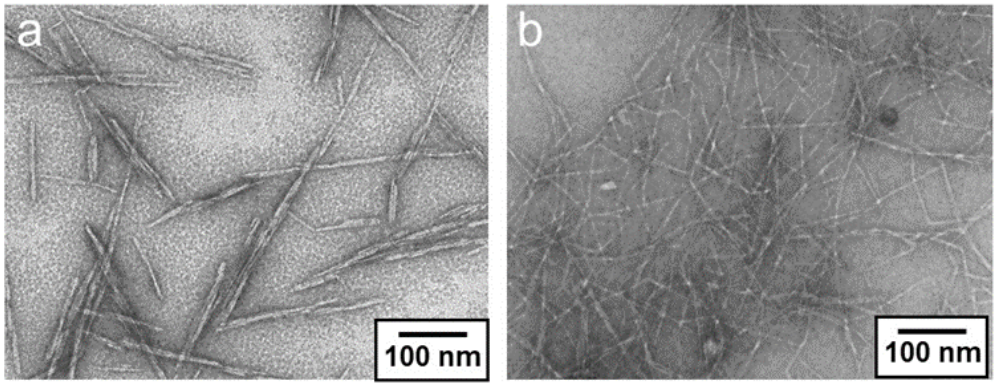

Figure 1—Micrographs showing notable differences in particle morphology between two CN types: (a) CNCs produced from the CNC pilot plant located at FPL (Reiner and Rudie 2013b); (b) CNFs produced using pretreatments from the CNF pilot plant located at FPL (Reiner and Rudie 2013a).

acknowledged that some valuable methodologies may have been missed herein.

The process of bringing research success to industrial utilization is difficult because it is fraught with barriers such as existing capital and processes, customer resistance to change, and suspicious attitudes toward new technology. This challenge is further exacerbated by the development of new materials that may not be "drop-in" ready for current industry manufacturing processes, as is the case of hydrophilic CNs added to hydrophobic polymer composites. Often new products, processes, and applications (customer acceptance) need to be developed to allow utilization of non-drop-in materials. Successful drop-in use of CNs requires hitting an extremely small bullseye. Thus, the low barrier of entry applications for new materials are niche and newly developed products. Given all these caveats, barriers, and restrictions, are there industrially viable CN composites? Fortunately, and excitingly, the answer is yes! Will industry therefore pick them up and run with them? The answer depends on a multifaceted techno-economic analyses landscape. A detailed discussion of this landscape is beyond the scope of this review. Briefly, consider that even if the new material meets the performance needs, is simple to implement (drop-in), and is cost-effective (does not decrease profit), there are many additional factors that need to be considered for marketability (e.g., competition, customer demands, and government regulations). Of particular interest for nanomaterials is the listing of a chemical or material by a regulatory body or law as being either allowed for use or banned. In the United States, the Toxic Substance Control Act (TSCA) (EPA 2021) regulates the use and import of chemicals and materials. The U.S. Food and Drug Administration (FDA) can grant a material generally recognized as safe (GRAS) status (FDA 2016) resulting in its regulatory barriers being substantially lowered. Even in the face of these challenges and more, many market segments undergo constant change. Therefore, there are frequent opportunities for new materials that meet the needs of the moment, or longer, to jump into the market.

In this critical review, CN polymer composites are reviewed in three categories: (1) waterborne, (2) freeze-dried, and (3) alternative. These categories refer to the process used in handling and preparing the CNs for incorporation into polymers or resins. In the waterborne process, CNs are dispersed or conveyed in water and incorporated into resins, etc., in a similar state. In the freeze-dried process, water is removed from the CNs, resulting in a CN powder that is subsequently incorporated into polymers or resins. Although freeze-drying is very time consuming, it is included in this review because it is an existing industrial process (e.g., instant coffee). There is potential for other faster drying methods to fill its place, such as spray-drying. Spray-drying was not incorporated as a separate category due to the low number of publications covering studies that used this method. Finally, the alternative category encompasses approaches that generally differ from the waterborne and freeze-dried approaches.

2. Results and Discussion

2.1 Waterborne Systems

Because most CN extraction methods handle the cellulosic starting material in water and the CN product output in the aqueous state, using these products directly without further modification is by default an easy path toward industrialization. Specifically, such an approach may be ideal for the coatings industry where waterborne (WB) products with low volatile organic content have replaced the majority of solvent-borne products, although this sacrifices mechanical performance to some degree. Hence, this market could potentially benefit from a WB reinforcing additive. Broad industrial application of such materials exists worldwide in the areas of WB protective coatings and

adhesives, which are markets on the order of billions of dollars in sales annually.

In 1995, the potential for CNs to provide significant beneficial reinforcement to a polymer matrix was demonstrated by the simple act of blending an aqueous CN dispersion with a WB polymer latex (Favier and others 1995a, 1995b). This was made possible by the use of sulfuric-acid-hydrolyzed tunicate, *Microcosmus fulcatus*, a sea creature harvested from the Mediterranean Sea. After treatment and acid digestion, they yield long and uniform tunicate CNCs (t-CNC). These were added by direct blending to a preformed styrene–acrylate latex, followed by air-drying for 21 to 30 days. This drying time was unusually long as most waterborne latexes dry within one day. This was probably necessitated by a large amount of water brought into the latex by the dilute CN. Nonetheless, this work is included in the review because its findings illustrate fundamental learnings that impact the rest of the body of work in this area. The resulting composite films exhibited an increase in shear storage modulus (G') below the glass transition temperature (T_g) that incrementally increased with t-CNC loading. Above T_g, where the matrix lost the majority of its stiffness, the composites exhibited orders-of-magnitude increases in modulus as the concentration of t-CNC increased from 1 to 14 wt%. At 14 wt%, the modulus was only slightly below the matrix's glassy modulus. This effect is demonstrated in their dynamic mechanical analysis (DMA) data (Fig. 2), where G' is plotted as a function of temperature for the matrix and CNC composites. Composites loaded with 6 and 14 wt% maintained their stiffness improvement to more than 100 K beyond the point where the matrix G' drops off significantly. Therefore, substantial and novel mechanical reinforcement abilities were demonstrated at an early stage in the CN research field (approximately 25 years ago). A transmission electron microscope (TEM) image of the 6 wt% composite demonstrates that the CNCs were well dispersed in the matrix (Fig. 3). The rapid rise in modulus above T_g was attributed to an interaction between t-CNCs facilitated by hydrogen bonds. A percolation model was proposed to explain this behavior in which these interactions are triggered when the concentration reaches a critical point such that an interacting network of CNCs occurs (Favier and others 1997). A key point of this early research and proposed model is that achieving a dispersion of individual CNs in the matrix is essential for optimal performance enhancement. This impacts the work subsequently discussed because agglomerated systems do not typically have such large increases in rubbery plateau modulus. Currently, t-CNCs are not known to be commercially viable because there is no current source harvesting them. However, they are included here to introduce CN reinforcement concepts.

The available literature provides examples that meet the criteria of this review and provide further exploration of WB

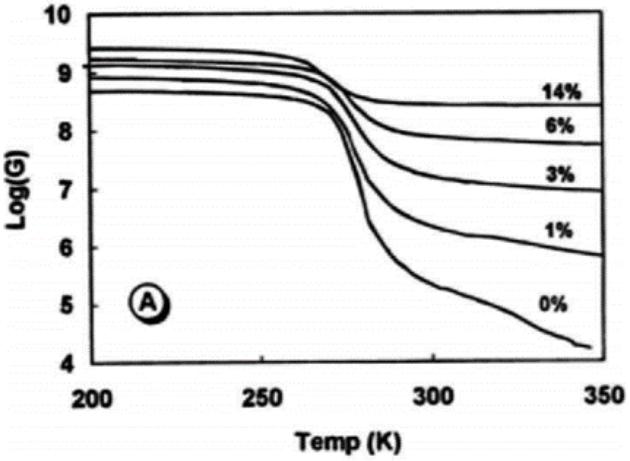

Figure 2—Plot of shear storage modulus versus temperature for matrix (0%) and composites up to 14 wt% t-CNCs as a function of temperature. The uniform dispersion of t-CNCs within the polymer matrix has a stiffening effect most notably above T_g (~275 K) (Reprinted with permission from Favier and others (1995b). Copyright 1995 American Chemical Society.)

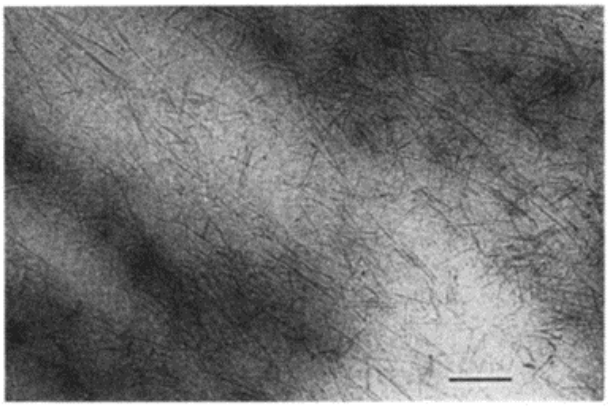

Figure 3—Transmission electron microscope image of 6 wt% t-CNC–latex composite illustrating uniform dispersion. Scale bar is 0.5 µm. (Reprinted with permission from Favier and others (1995b). Copyright 1995 American Chemical Society.)

polymers reinforced with a variety of CN. Sampling mechanical property data from this subset of literature potentially allows comparison of methods, CN types, matrixes, and results. Rather than considering the studies independently, we can consider them collectively, making it possible to identify any fundamental principles and mechanisms in the reinforcement effect of CN additives in polymer matrixes. This is accomplished by comparing the ratios of the rubbery plateau moduli (E_{RR}) (ratio of composite to matrix) and comparing the tensile moduli (E_R) as shown in Figures 4 and 5, respectively.

The rubbery plateau modulus ratio data in Figure 4 are separated into two distinct profiles or groups. The top group labeled as "upper" exhibits orders-of-magnitude increases in

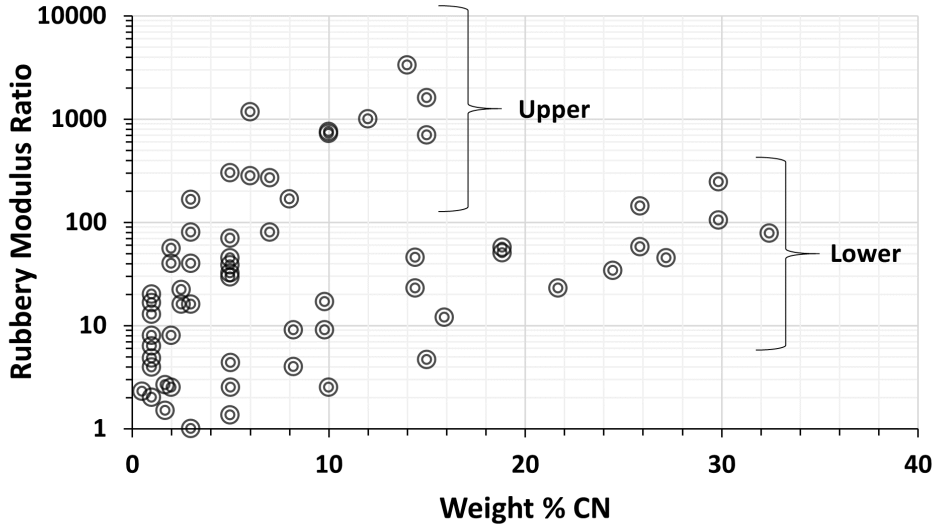

Figure 4—Plots of rubbery modulus ratio (E_{RR}) of waterborne CN composites at $T > T_g$. Data taken from literature referenced in Table 1.

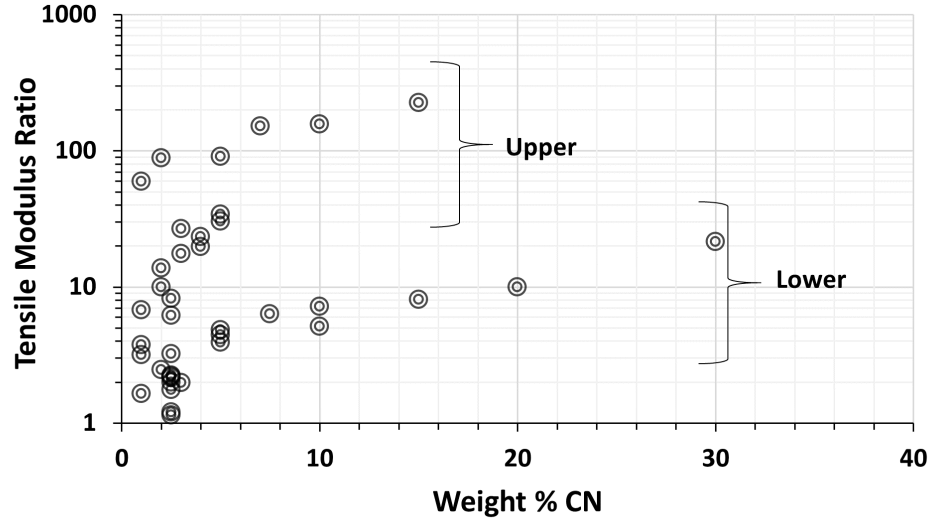

Figure 5—Plot of tensile modulus ratio (E_R) versus wt% for CN waterborne polymer matrix composites at ambient temperature (20 to 25 °C). Data taken from literature referenced in Table 1.

modulus ratio with CN content, reaching three orders of magnitude at 10 wt%. Certainly, this is an impressive capability of CN. They can almost completely eliminate softening above T_g for a variety of polymers, as shown in Figure 2 and described in Table 1. The industrial advantage gained by successful utilization of such an effect should be quite substantial. Benefits include increased heat deflection temperature and product use temperature range. The bottom group labeled as "lower" also has notable mechanical property improvements that provide one order of magnitude and two orders of magnitude increases in modulus ratio with 10 and 30 wt% CN additions, respectively. The lower reinforcement per added CN amount for the lower group may have been associated with CN agglomeration or a diminished CN–matrix polymer interaction, thereby compromising load transfer. The use of agglomerated nanomaterials is akin to using a larger size–scale variant. As the reinforcing phase increases in dimension, the interfacial contact area between the reinforcement and the polymer matrix decreases and thus it becomes less effective. Nonetheless, this lower group of composites still have mechanical property improvements that provide 100 times increase in the composite's rubbery plateau modulus at a 30 wt% loading. Arguments for and against full dispersion

Table 1—Summary of moduli ratios and fabrication approaches for waterborne cellulose nanomaterial (CN) composites

Matrix[a]	CN[b]	Dispersion[c]	Max E_{RR}[d]	Max E_R[d]	Approach
			Latex		
SBA	t-CNC	D	$3{,}333^+$		Not disclosed, 21-30 d drying (Favier and others 1995b)
Acrylic	CNC	?	168^+	–	Magnetic stirrer, rotovap[e], 2.5-3.5 d drying (Ben Mabrouk and others 2012)
Acrylic	CMF	?	$1{,}600^+$	–	Magnetic stirrer, rotovap, 2.5-3.5 d drying (Ben Mabrouk and others 2012)
NR	CNF	?		7.1^-	Bead mill/sonication, 1 d oven-drying (Abraham and others 2012)
SBR	CNC	D	245^-		3 h stirring, 1 h sonication, 2-3 d oven-drying (Annamalai and others 2014)
Acrylic	CNF	A		2.2^-	30 min disperser mixing, 1 d ambient drying (Gruneberger and others 2014)
NR	CNC	S	45^+	3.9^-	4 h magnetic stirring, 12 h 60 °C/15 m 100 °C (Zhang and others 2014)
NR foam	CNF	A	5^-		"Vigorous" mixing, dry, 2-roll mill, cure 145 °C (Chen and others 2015)
SEHA C+	CNF	A	23^+		Mechanically stirred, 2 d oven-dry ~40 °C (Nechyporchuk and others 2016)
SEHA A–	CNF	D	19^+		Mechanically stirred, 2 d oven-dry ~40 °C (Nechyporchuk and others 2016)
NR	CNC	S	29^+	30^+	4 h magnetic stirrer, 12 h oven-dry 40 °C (Neto and others 2016)
SBA	CNF	?	755^+	224^+	Not disclosed (Khiari 2017)
PE	CMF	A		21^+	5 min blending, 24 h oven-dry 60 °C (Maia and others 2017)
			Emulsion (liquid particles)		
SEHA	CNC	D	300^+		Silylation, mini-emulsion, stirred, 1 d 40 °C (Ben Elmabrouk and others 2009)
Epoxy	t-CNC	D	39^+		Not disclosed, oven-dry 6 h 40 °C and 4 h 80 °C (Ruiz and others 2000)

[a]SBA, styrene butylacryate; SBR, styrene butadiene rubber; NR, natural rubber; SEHA, styrene ethyl hexylacrylate; PE, polyethylene.
[b]t-CNC, tunicate cellulose nanocrystals; CNC, cellulose nanocrystals; CMF, cellulose microfibrils; CNF, cellulose nanofibrils.
[c]State of dispersion: D, dispersed; A, agglomerated; S, sedimented; and ?, unknown/uncharacterized.
[d]"+" denotes the value is in the upper group and "–" denotes the value is in the lower group in the modulus ratio plots.
[e]Rotovap stands for rotary evaporator.

at the nanoscale come down to a rationalization between the expense of establishing such a dispersion versus the value of the benefit derived from it. The other factor is that fully dispersed CNs typically increase viscosity substantially with higher loadings, a phenomenon that is dependent on aspect ratio, particle morphology (e.g., degree of branching), dispersion, and applied shear. Lastly, it should be noted that there was no clear trend of CN type being predominate within either upper or lower groups.

Because most polymers lose a vast majority of their stiffness above T_g, the values of the rubber plateau modulus ratios can be quite large because of the greater effect reinforcing phases have on low modulus materials. This is most evident at high concentrations of CN where it's possible to reinforce the rubbery state to such an extent that little if any drop in modulus occurs. Additionally, the subjective choice of what temperature to use for the comparison can have a substantial effect on the magnitude of the rubbery modulus ratio. Tensile modulus comparisons should offer a more concrete evaluation. One major issue is that the literature is quite varied in its characterization methods such that not all conduct DMA, tensile testing, or either. Typically, the addition of CNs increases the modulus, tensile strength, and often impact strength of the polymer, whereas elongation to failure is decreased. In addition to the modulus reporting literature subsequently discussed, five other publications are cited here because they met the criteria of the review but did not report modulus (Cao and others 2013a, 2013b; Cataldi and others 2015; Sanches and others 2014; Thomas and others 2015). When the tensile modulus ratios are examined (Fig. 5), two differentiated groups of data are observed in a similar manner as the rubbery plateau modulus ratio. These are labeled in the same way with the likelihood of agglomeration affecting the lower group. The large reduction in the tensile modulus ratio values compared with the rubbery plateau modulus ratios illustrates the phenomenon of reinforcing phases having a larger relative effect on low modulus materials. This factor is also present in the tensile modulus ratios, shown by the fact that some of the very high values in Figure 5 are from CNs added to low modulus polymers.

Bearing this in mind, the tensile modulus ratios indicate that CN polymer composites can reasonably expect to reach a modulus improvement of 10 to 100 times. In perhaps a less optimal CN composite, the tensile modulus ratio improvement will reach only approximately 10 times. How does this compare to industrially used reinforcement phase materials? Unfortunately, none were included in the literature for comparison. This appears to be an area of substantial deficiency that may be a barrier for industrial interest. Additionally, given the diversity of monomers and monomer ratios that can be used in synthesizing latex polymers, one cannot simply check the literature for comparisons. This requires researchers to include currently used industrial reinforcing materials alongside their evaluation of CN composites.

The key question is then, what methods or parameters are necessary for CN composites to be in the upper group or in the lower group in Figures 4 and/or 5? Hopefully, an examination of the selected literature should reveal best practices and identify others that need improvement. Note that based on the selection criteria for this review, all the methods to be discussed did result in notable reinforcement as evidenced by Figures 4 and 5 and many other properties such as strength. The WB CN composite literature selected for this review with modulus data is concisely summarized in Table 1, which also reports the maximum value obtained in modulus ratio for a given material combination and composite processing approach. Each entry in Table 1 provides the matrix, CN type, maximum rubbery modulus ratio, maximum tensile modulus ratios, and the approach used in fabricating the composite. Notations within the matrix column indicate whether the CN was dispersed, agglomerated, sedimented, or uncharacterized, while notations in the maximum modulus ratios column denote if the values were in the upper or lower grouping. When looking at all of the studies to assess which material types and processing approaches result in the higher mechanical properties, it is interesting to note that all but one of the composites known to have a dispersed CN phase were in the upper group in agreement with common perception that dispersion results in the greatest property enhancements. The composites known to be agglomerated fell half in the upper and half in the lower giving a mixed result. The composites with unknown dispersion state are noted as such because the researchers did not report this or did not provide images sufficient for a determination to be made. Overall, the assumption that good dispersion results in higher mechanical properties is supported here but cannot be definitively confirmed because of the lack of overwhelming data, the brevity of dispersion method descriptions, and generally inconsistent dispersion characterization in the final matrix polymer. Additionally, there was insufficient detail on blending methods to make a conclusive statement regarding which composite fabrication approaches were more likely to produce composites with higher mechanical properties. In general, approaches such as dilute/low shear or high shear mixing are preferred to disperse CNs because of the need to interrupt strong self-affinity of the CNs. Dilution of CNs is an effective means to reduce viscosity and facilitate blending with polymer lattices with the tradeoff being long drying times.

There is more knowledge to be gleaned from this collection of WB CN composite literature. Four studies are subsequently described in greater detail to highlight other aspects of CN dispersion and incompatibility issues. The effect of degree or configuration of CN dispersion within a matrix polymer on mechanical properties was reported by Annamalai and others (2014). They fabricated CNC–SBR (styrene-butadiene rubber) composites via relatively high shear mixing and long drying times. TEM imaging showed the CNCs to be fully dispersed within the matrix. The composites exhibited large gains in glassy and rubbery modulus with increasing CNC loading. The ratios, however, were in the lower group because of the relatively high rubbery plateau modulus of the SBR. A second step of processing was applied to a portion of the films. These samples were placed in a compression molder at 120 °C for 15 min with thickness controlling blocks. This processing reduced gains in rubbery plateau modulus, thereby suppressing the modulus ratio for the resultant composites. This phenomenon was evaluated further by creating an acetone–CNC gel via slow solvent exchange. This was combined with SBR dissolved in acetone. After removal of the acetone, the composite was compression-molded as previously described. These composites had the lowest gains in modulus of the three. The researchers illustrated the change in CNC distribution in the composite (Fig. 6) as an even distribution of CNCs between latex particles for the aqueous-derived composite, a similar yet compacted state for the compression-molded composites, and as a mixture of dispersed, compacted, and agglomerated CNCs for the solvent-exchanged state, which was supported by TEM images. These experiments illustrate that there appears to be an optimum spacing for CNC–CNC interactions or between CNC-reinforced domains that can be interrupted by compaction and other effects that act to disrupt or constrain

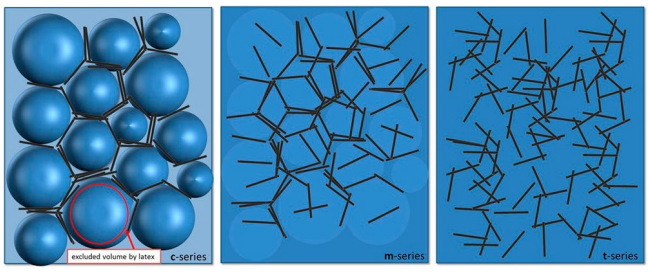

Figure 6—Conceptual schematics of CN networks dispersed around latex (left), compacted (center), and compacted with some agglomerates (right). (Reprinted with permission from Annamalai and others (2014). Copyright 2014 American Chemical Society.)

it. This optimum seems to exist where individual CN fibers or isolated bundles act to reinforce the matrix, and then these reinforced domains are able to interact with adjacent reinforced domains upon reaching sufficient concentration. High degrees of dispersion should reach this point at lower concentrations. This is evident in Figure 4, which shows that some composites reached a times 10 improvement in rubbery modulus at concentrations of 1 wt% or less whereas others required 10 wt%.

Evaluating the benefits of CN in water- and oil-based wood coatings, Gruneberger and others (2014) added CNFs into eight commercial latex coatings illustrating the difficulty of dispersing CNs into hydrophobic systems. The latices consisted of three acrylics, one acrylic–styrene, one acrylic–alkyd–oil, and three alkyd–oil coatings. The CNF aqueous dispersion was added to the coatings after formulation components were incorporated via 30 min of mechanical mixing with a disperser blade. The films were dried under ambient conditions for one day then removed from the supporting substrates and stored until tested. Overall, this process closely simulated commercial handling and the expected drying period. The CNFs formed uniform coatings with dispersed agglomerates, per SEM, in the four acrylic formulations but formed highly agglomerated and rough films in the alkyd–oil formulations. The alkyd–oil with CNF composites required a compression molding treatment to homogenize their irregular surfaces. Mechanical behavior was characterized by tensile data. Modulus ratios for the eight composites with 2.5 wt% CNFs ranged from 1 to 8 with the most significant factor for increasing modulus ratio being lower modulus of the matrix rather than state of dispersion.

Dispersion instability and perhaps incomplete compatibility was observed by two research groups during drying of natural rubber (NR) latexes that resulted in sedimentation of CNCs (Neto and others 2016, Zhang and others 2014). Sedimentation resulted in the upper layer being low and the bottom layer being rich in CN concentration. This was clearly evident in an SEM micrograph of a cross section (Fig. 7) and was confirmed by FTIR. Sedimentation was most pronounced and detrimental at lower concentrations and eased at 5 wt%. The cause may be a rapid increase in the hydrophobic nature of NR during drying, too low of a viscosity to hold the CN in dispersion, or other yet to be elucidated cause. Both CNCs used in the cited research were extracted with sulfuric acid and should have been self-emulsifying. Because CNs have a refractive index similar to most polymers, such CN sedimentation may go unnoticed except when composites are examined in cross section.

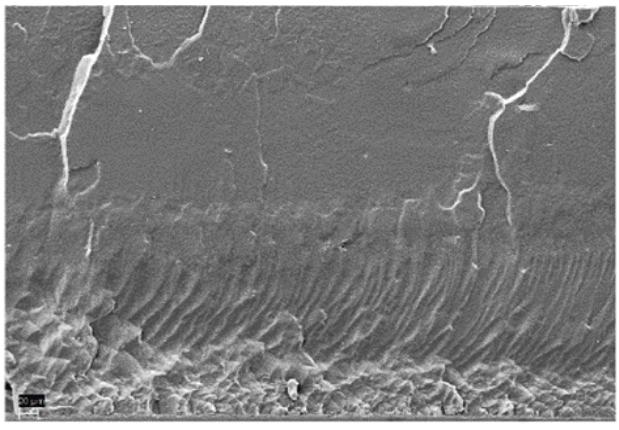

Figure 7—Natural rubber latex film with 2 wt% CNCs with a CNC-rich bottom layer and CNC-poor top layer due to sedimentation. CNC scale marker is 20 µm.

Nechyporchuk and others (2016) blended NaOH-neutralized TEMPO-oxidized CNFs with anionic and cationic surfactant-stabilized latices of styrene ethyl hexylacrylate (SEHA) demonstrating the impact of ion–counterion effects. The cationic latex resulted in gross phase separation of CNFs within the matrix, whereas the anionic latex produced uniform dispersions. The cationic latex films required brief hot pressing at 90 °C to smooth out their surfaces for test specimen preparation. The positively charged surfactant on the emulsion particles appears to be acting as a multivalent cation that strongly coordinates to negatively charged TEMPO-oxidized CNFs in a fashion similar to adding Ca^{+2} results in gross phase separation. This phenomenon may explain why a commercial latex is surprisingly found to be incompatible with ionically charged CNs when the surfactant chemistry is unknown. The cationic latex's modulus was an order of magnitude lower than that of the anionic. CNs reinforced both despite the phase separation resulting in both systems having high modulus ratios, which put them in the upper group. Ben Elmabrouk and others (2009) had similar issues with a latex becoming unstable upon addition of CN. Their solution was to silane-treat the CNs prior to adding them to the latex, and this greatly improved stability. The silane, which is attached to the surface of the CNs, may be acting as a screen between the ionic groups on the surface and the surfactant, thereby avoiding agglomeration.

2.1.1 Consequences and Misconceptions

A factor to consider for all systems discussed in the preceeding section is that since they were all WB, they continue to have an affinity for moisture uptake even in the dried or cured state as the surfactants remain in the matrix. Adding unmodified CNs to these matrixes could have a substantial effect on their moisture uptake. Annamalai and others (2014) evaluated the moisture uptake of SBR–CNC composites processed via three different methods: casting, molding, and acetone gel templating. As anticipated, the matrix absorbed considerable amounts of moisture with the absorption rate increasing with CN additions. The total amount of moisture absorbed by the composites was a strong function of the CN loading and processing method. Both the cast and molded specimens had moisture uptake

higher than or similar to the matrix at low loadings of CN. The total moisture uptake decreased with higher CN loadings and in some cases fell below that of the neat matrix. The acetone gel template composites and matrix behavior indicated that the surfactant had been reduced or removed by the acetone such that the moisture uptake was reduced tenfold. Further studies of the change in modulus after water immersion were conducted indicating a linear drop in modulus down to a stable lower value at saturation. After drying, the modulus was found to recover completely. Looking at moisture vapor in the form of humidity exposure, Sanches and others (2014) exposed polyurethane (PU) latex–CNF composites to 30% and 60% relative humidity (RH). No moisture absorption or detriment was observed at 30% RH for both the matrix and composite. In contrast, the 60% RH exposure caused the matrix to absorb 1.5 wt% moisture. This increased with CNF addition to a maximum value of 2.2 wt% with 30 wt% CNF in the composite. Moisture uptake reduced strength of the matrix and composites and increased the elongation to failure, overall having a plasticization effect. This plasticization effect lessened as CNF loading increased to 30 wt% such that more strength was retained. These studies indicated that CN can have both negative and positive effects on moisture uptake and its effects on composite performance.

A common misconception found in literature is that if composite films are transparent, the CNs must be well dispersed in the matrix. Since the refractive index of CNs matches most polymers, their presence does not render them opaque or translucent unless the phase-separated domain size exceeds the wavelength of light. Therefore, transparency is generally maintained to a high degree. Thus, in WB polymers, transparency should be maintained with agglomeration examined via a facile technique such as polarized optical microscopy or simply a visual examination with the samples back-lighted and viewed between cross-polarized films. A uniformly dispersed CN composite will typically give a glowing appearance proportional to the CN loading. A phase-separated composite will have numerous bright white to colored domains coincident with agglomerates. Girouard and others (2015) studied CNC-reinforced WB epoxy composites using low shear mixing methods. They evaluated the effect of addition of all three composite components at once (one-step process) versus premixing of the epoxy and aqueous CNCs prior to amine addition (two-step process). After allowing the blended systems to precure for 1 to 3 h depending on water content, they were cast as films and cured for 2 h at 100 or 120 °C for higher CNC loadings. All of the films were transparent, yet examination under cross-polarized light revealed that the composite created by an all-at-once addition had numerous CNC-rich domains, whereas the two-step mixing had fewer domains that were significantly more diffuse (Fig. 8).

2.1.2 Summary

It is clearly evident that CNs can boost stiffness and tensile strength of WB latex and emulsion polymers that are widely used in the coatings and adhesives market segments. Because CNs are commonly produced in a water dispersion, they are suitable for drop-in addition in such products. The extra water they bring into the formulation must be accounted for or they need to be added at a more concentrated state. Strong affinities exist between oppositely charged CNs and ionic surfactants that result in gross phase separation and irregular films. Use of a nonionic surfactant or one that has the same ionic charge as the CN, typically negative, avoids this issue. DMA-based rubbery modulus measurements appear to be useful in evaluating the state of the CN dispersion and changes in it caused by processing steps or other effects. Gaps exist in this research field because of the lack of comparisons versus industrially used reinforcing phases and experimentation that better correlates mixing methods, initial CN dispersion, CN dispersion in the composite, and final composite properties. Garnering industrial interest may be facilitated by such results. Perhaps a gap that affects the CN–composite field in general is the lack of proper characterization of the CN after extraction and surface modification as well as their state of dispersion in the composite (Foster and others 2018). In transparent polymers, the latter is easily handled by use of polarized optical microscopy. If the matrix polymer is not transparent enough to visible light, then an artifact-free cross section of the sample should be made and morphology should be evaluated by atomic force microscopy (AFM) or electron microscopy.

2.2 Freeze-Dried Systems

In efforts to move toward more hydrophobic polymer composites, researchers have endeavored to separate CNs from the aqueous medium and transform or compatibilize their hydrophilic surfaces. Freeze-drying is a method that imposes rapid cooling to CN aqueous dispersions such that ice crystal growth is minimized or controlled. Once frozen, the water is removed via vacuum-assisted sublimation with heat added optionally to increase the rate of water removal. What remains is a white powder of dry CN in a more or less redispersible form depending on many factors. CNCs can be redispersed directly in hydrophilic medium with the assistance of high intensity mechanical and/or ultrasonic energy. CNFs and larger CN types typically require intense mechanical shear to disperse because the freeze-dried (FD) agglomerates tend to be strongly hydrogen-bonded and physically entangled. The methods used to modify and disperse FD CNs are quite varied; therefore, a seminal or typical work is not presented as a summary or introduction as was available for WB composites. Instead, the tensile modulus ratios are presented in a linear scale in Figure 9 as extracted from the literature summarized in Table 2. Glassy storage modulus, E' or G' at $T < T_g$, ratios are included in

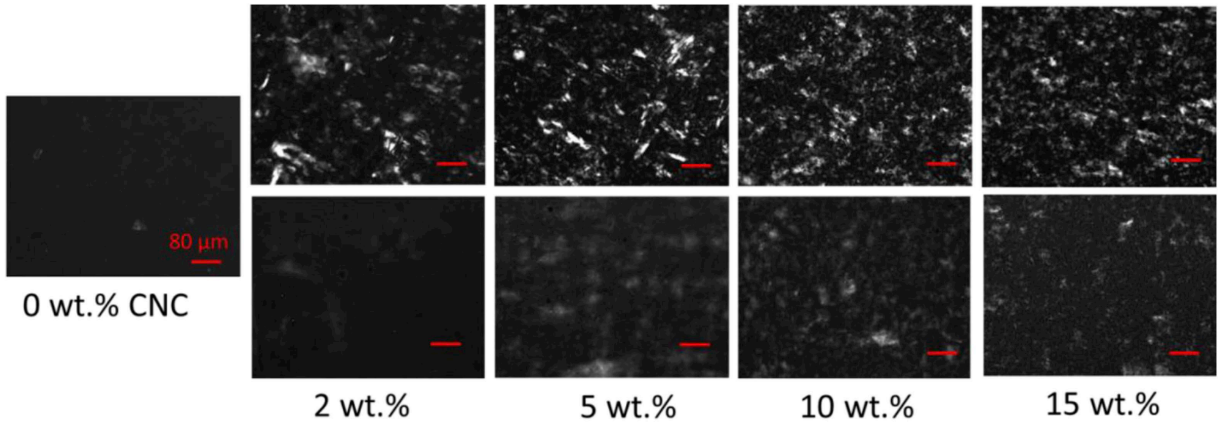

Figure 8—Polarized optical micrographs of CNC waterborne epoxy films produced by the one-step process (top) and two-step process (bottom). (Reprinted with permission from Girouard and others (2015). Copyright 2015 Elsevier.)

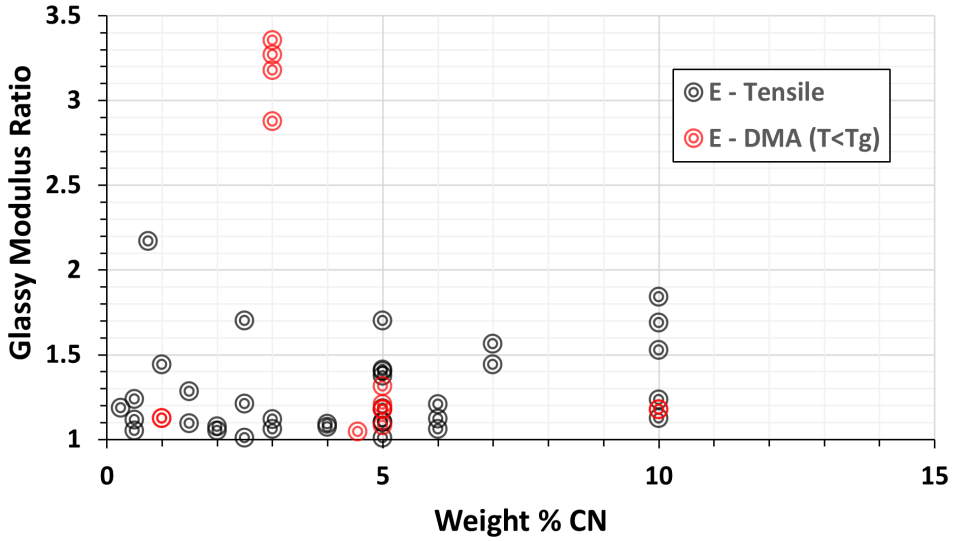

Figure 9—Plot of tensile and dynamic mechanical analysis (DMA) storage modulus data from freeze-dried CN composites. Data taken from literature referenced in Table 2.

Figure 9 because many references do not provide tensile data. Modulus ratio values for these composites were lower than those for the WB composites presented in Table 1 and Figures 4 and 5. A factor in the lower modulus ratios is that starting with FD CN hampers the removal of all agglomerates and the establishment of a nanoscale dispersion. Thus, the results are probably suppressed from the ideal state because of agglomeration or nonideal distribution of CNs within a reinforcing network. This was discussed in Section 2.1 (Waterborne Systems) and illustrated by research that demonstrated that reduction in the degree of dispersion diminished properties (Fig. 6) (Annamalai and others 2014). Another factor contributing to the lower modulus ratios is the fact that FD CNs are used to reinforce polymer with higher moduli than that used in the WB latex composites in Section 2.1. Reinforcing phases generally have a proportionally greater impact on low modulus polymers.

All of the studies from the literature that met the criteria for this section and also reported modulus data are summarized in Table 2. In addition to modulus improvements, tensile strength and many other properties are improved with addition of CNs to hydrophobic polymers. These property improvements will be briefly reviewed when the top five performing composites, shown in bold in Table 2, are discussed. Table 2 is divided into groups based on additives or surface modifications used. In addition, Table 2 lists the matrix, CN type, maximum modulus ratio (tensile or DMA at $T < T_g$), and an abbreviated description of the approach used to fabricate the composites. The first group of composites are those made with no additives or surface modification in hydrophobic polymers. These composites

Table 2—Summary of freeze-dried cellulosic nanomaterial (CN)–polymer composite performance and production approaches[a]

Matrix	CN[b]	Max E_R or E_{RR}	Approach
		No additives or surface modification	
PP	CNC	1.4	Sprayed into LN_2, FD, melt blend (Khoshkava and Kamal 2014)
Epoxy (DGEBA)	CNF	**2.2**	High speed shear into epoxy (Saba and others 2017)
LDPE	CNF-cotton	**1.8**	TSE blending (Farahbakhsh and others 2015)
PP and LDPE	CNC	1.5 and **1.7**	Cold high intensity shear/kneading SSSP (Iyer and others 2015)
		Compatibilizer added	
Iso–PP/MAPP	L-CNF	1.1	120 °C batch kneading SSSP (Iwamoto and others 2014)
PLA/surfactant	CNC	1.2	CNs blended with surfactant, FD, TSE (Bondeson and Oksman 2007)
PLA/surfactant	CNC	**1.8**	CNs blended with surfactant, FD, TSE (Fortunati and others 2012)
PLA/PEO	CNC	1.1 (0% PEO)	CNs blended with PEO, FD, melt-mixed (Arias and others 2015)
HDPE/PEO	CNF	N/A	CNs blended with PEO, FD, melt-mixed (Li and others 2014)
PU/PTMEG	CNF	1.1	CNs blended with PTMEG, dried, TSE, annealed (Amin and others 2016)
HDPE/PEO	CNC	1.3	CNs blended with PEO, FD, ground, TSE (Inai and others 2018)
PLA/MAPLA	CNC	1.04	FD CNs added to melt mixer (Hong and Kim 2013)
		Silane surface modification	
UPR/LNR	CNC	1.2 (w/o silane was higher)	CNs silane treated, FD, blended in styrene then added to UPR/LNR (Kargarzadeh and others 2015)
Bio-epoxy	CNC	1.2 (w/ or w/o silane)	CNs silane treated, CF, FD, heated, sonicated in epoxy and amine (Yue and others 2018)
PLA	CNF	**3.3** (methacryloxy)	CNs silane treated, CF, FD, heated, extruded, injection-molded, annealed (Raquez and others 2012)
		Surface modification during extraction	
PLA	CNC	1.3 (lactic acid)	CNs extraction w/ acid blends, FD, TSE blended (Spinella and others 2015)

[a] PP, polypropylene; DGEBA, diglycidyl ether of bisphenol A; LDPE, low density polyethylene; iso-PP, isotactic PP; MAPP, maleic anhydride functionalized PP; PLA, poly(lactic acid); PEO, poly(ethylene oxide); HDPE, high density polyethylene; PU, polyurethane; PTMEG, poly(tetramethylene glycol); MAPLA, maleic anhydride functionalized PLA; UPR, unsaturated polyester resin; LNR, liquid natural rubber; CNC, cellulose nanocrystals; CNF, cellulose nanofibrils; L-CNF, lignin-coated CNFs; LN_2, liquid nitrogen; FD, freeze-dried; TSE, twin screw extruder; SSSP, solid state shear pulverization; CF, centrifuged.
[b] All CN source materials were wood biomass unless noted otherwise.

were made possible by innovative and brute force methods. Surprisingly, two of the composites in this category are within the top five performing composites. In the second category, an intermediary substance was added to bridge the gap in surface energy between the matrix and CN. The compatibilization strategies included functionalizing the polymer backbone for reactivity–compatibility between cellulose and maleic acid or addition of a surfactant or various molecular weight polyethers. The composites resulting from this strategy generally have low modulus ratios because of plasticization effects. An exception was one of the poly(lactic acid) (PLA)–surfactant CNC composites, which had a relatively high ratio of 1.8. Remarkably, another composite in the same category was identically prepared and processed but resulted in a lower modulus ratio. This will be examined in detail in the next paragraph. The third category is silane surface modification of CNs for compatibility and potential reactivity with the matrix. This approach is widely used at industrial scale, typically on inorganic materials; however, its use with cellulose is not as straightforward, which will be subsequently discussed. The final category is surface modification during extraction. This strategy takes advantage of the residual acid ester that remains after cellulose is hydrolyzed to facilitate compatibility and, in this instance, was the most facile method found.

The first three of the top five performing composities, bold in Table 2, are those that used high shear to create CN composites with no dispersing additives. Saba and others (2017) combined FD CNFs with an epoxy resin, DER 331 (DGEBA), via an undescribed high speed mechanical process. This was combined with an amine hardener in a mechanical mixer for 20 min, and composites were fabricated at various loadings of CNFs via a hand layup

process. A loading of 0.75 wt% CNF resulted in improved modulus, tensile strength, elongation to failure, and impact strength. TEM imaging revealed well-dispersed groupings of material in the epoxy. They did not appear to be fibrous. Thus, it is unclear if they were small agglomerates or bundles of fibers. Overall, it is an impressive result from direct-blending of CNFs into epoxy resin with no surface modification. The lack of details on the mixing method is unfortunate. Farahbakhsh and others (2015) blended FD CNFs from various sources with powdered low density polytheylene (LDPE) in a lab-scale twin screw extruder (TSE) at 170 °C. Softwood pulp CNFs had minimal effect on mechanical properties, whereas recycled cotton CNFs notably increased the modulus while slightly increasing tensile strength and decreasing elongation to failure with higher loading. Solid state shear pulverization (SSSP) at –7 °C was used by Iyer and others (2015) to codisperse LDPE or polypropylene (PP) with FD CNCs in the solid state without thermal degradation. SSSP exposes materials to high shear and compressive forces resulting in repeated diminution of large particles and agglomerates. CNs and polymer fractions are then forced back together under compression. The resulting powder was compression-molded to create tensile specimens. Melt mixing via a TSE was evaluated as a direct comparison and to determine the stability of the SSSP dispersion. CNC–LDPE composites had increased modulus and tensile strength while maintaining elongation to failure. In contrast, TSE-processed composites exhibited notably lower increases and sharply reduced elongation. The CNC–PP composites behaved similarly although with lower overall improvements and sharply reduced elongation. The SSSP 5 wt% CNC composites were processed again with TSE at various temperatures. At 175 °C, the modulus ratio was reduced to 1.3 from 1.4 with darkening in color of the composite. Modulus ratios continued to fall as processing temperatures increased, illustrating the need to address the thermal instability of acid-extracted CNCs via antioxidants or other means (Espinosa and others 2013, Kargarzadeh and others 2012, Yu and others 2013).

Compatibilization is the addition of one or more additional components to the composite that have chemical attributes of the matrix and the dispersed phase. These are typically used when the dispersed phase has some degree of incompatibility with the matrix. Thereby the compatibilizer should end up at the interface between the dispersed phase and the matrix, improving dispersion and mechanical performance as a result. Fortunati and others (2012) blended aqueous CNCs with the surfactant Beycostat A B09, an acid phosphate ester of ethoxylated nonylphenol, and then conducted freeze-drying to remove water. The FD surface-modified CNCs (s-CNCs) were combined with PLA in a lab-scale TSE operating at 185 °C and then compression-molded into films at 200 °C. Composites contained 5 wt% s-CNCs and 5 wt% surfactant. The composites exhibited a significant increase in modulus, almost double that of PLA. Other tensile properties remained relatively the same except elongation to yield and break, which both decreased. Bondeson and Oksman (2007) followed a similar procedure for modifying CNCs with Beycostat A B09 with much lower increase in modulus. One difference between the two approaches was the grade of PLA with the former using Ingeo™ 3051D injection molding grade PLA (NatureWorks, Plymouth, Minnesota, USA) with 4% D-lactide and the latter using Ingeo™ 4032D biaxial-oriented film grade PLA with 2% D-lactide. 3051D has been discontinued, and the manufacturer's technical data sheet is no longer available. Other sources describe its use temperature as 55 °C (Jamshidian and others 2010) and elongation to failure as 2.5% (MatWeb 2019). Similar data for grade 4032D is 155 °C (Jamshidian and others 2010) and 100% to 180% (NatureWorks 2019), respectively. Thus, the 3051D grade that responded notably better to the same processing apparently has lower crystallinity and is more of a brittle material. Perhaps this is an example of a weaker polymer responding more positively to reinforcement or plasticization from the surfactant alleviating its brittle nature.

Silanization works so effectively in industry practice that its use in CNs would seem to be a given success. However, this was found not to be the case. In 2008, Lu and others (2008) silylated CMFs and found that the silane remained in the water phase during solvent exchange from water to acetone. They referenced a study that quantitatively characterized reactions between silanes and cellulose while casting much of the literature on the topic in doubt. Specifically, Gandini and Belgacem (2005) found that "claims to the actual occurrence of these grafting reactions are often unsubstantiated". Looking at the reaction between silane directly (RSi-OR) or with its hydrolyzed silane oligomers (RSi-OH), they stated that only the latter had been elucidated. Specifically, Valadez-Gonzalez and others (1999) found that reactions between cellulose in the solid state and hydrolyzed silanes proceed at useful rates only at temperatures exceeding 70 °C. Gandini and Belgacem (2005) studied silane reactions and summarized their findings and those of Valadez-Gonzalez and others (1999) as (1) RSi-OH forms strong hydrogen bonds with cellulose in water that easily disassociate upon washing, (2) RSi-OH–cellulose hydrogen bonds can be condensed if heated to more than 100 °C, and (3) RSi-OR in the presence of dry cellulose (i.e., in a hydrophobic solvent) will not react unless water is added. Therefore, it is apparent that reactions between cellulose and silanes are not as facile as with inorganic materials and require careful practice to create the hydrogen-bonded state with the oligomer and then condense it to a covalent bond after significant heating. Unfortunately, the authors did not offer a hypothesis or explanation for the difference in silane reactivity between cellulose and inorganic hydroxyls. Considering this issue here, it may be

possible that the extensive hydrogen bonding within cellulose lowers the basicity of its hydroxyls. The challenge then is how to condense silanes on cellulose. Can this be carried out in boiling water, or does one have to execute a careful and time-consuming solvent exchange as Lu and others (2008) undertook? There are two silane-treated CN composites described in Table 2 that were heated at 110 °C after treatment. Both studies carried out silane treatment in acidic aqueous conditions, concentrated and washed the products with centrifugation, and isolated the products via freeze-drying. The washing steps after centrifugation may have removed much of the hydrogen-bonded silane. The PLA composite demonstrated a times 3.3 increase in modulus, whereas the bio-epoxy composite was the same with or without silane (Raquez and others 2012). The difference appears to be that the former achieved a 1% degree of substitution whereas the latter had spectroscopic evidence of functionalization but no degree of substitution data. Therefore, there appears to be a gap in effective use of silanes on CNs brought about by the contradiction of needing to carry out silane hydrolysis and absorption in water with condensation taking place at or above the boiling point of water. Perhaps by developing an approach that achieves condensation without lengthy solvent exchange, CN composites may fully benefit from silanes.

Freeze-drying approaches are an effective means of water removal allowing further treatment of CNs for improved incorporation into hydrophobic polymers. This methodology facilitates the investigation into how well CNs perform as reinforcing phases in such materials. The poor redispersment of CN agglomerates derived from freeze-drying results in generally suboptimal composite performance. Addition of non-surface-modified CNs to hydrophobic polymers or resins can provide moderate benefits. The use of surfactants and polyethers appears to improve compatibility at the expense of stiffness. Silane surface modification of inorganic materials and their direct addition to adhesives, sealants, coatings, etc., for adhesion promotion is carried out routinely on a large industrial scale. Their use in cellulose is not straightforward due to a lack of a facile process to fully condense absorbed silanol oligomers. This challenge indicates that the full benefits from silane surface modification of CNs may not have been evaluated yet. Looking beyond modulus, the composites presented in this section displayed many more benefits such as enhancements in tensile strength, crystallinity, heat deflection temperature, crystallization rate, and more.

2.3 Alternative Methods

This third section presents methods that are alternatives to the use of CNs in WB polymers–resins or freeze-drying to remove water in a way that hopefully retains dispersibility. These approaches are quite varied with many providing alternative approaches to extraction and dewatering during compounding and surface hydrophobization from the aqueous state, with many, but not all, examining the impact on composite performance. Thus, the methods cannot be compared based on composite performance alone. We start by looking at surface modification approaches that take place simultaneously with extraction of CNs from biomass. These methods present an efficient approach to imparting desired surface functionality without further chemistry. This can be accomplished by using a mixture of organic and mineral acids during the hydrolysis stage. Examples include acetic or lactic acid mixed with HCl (Braun and Dorgan 2009, Spinella and others 2015) and a butyric acid–HCl blend (Braun and Dorgan 2009), which both result in CNs having the associated ester substituted on its surface. CNCs extracted with a blend of lactic acid and HCl and used to reinforce PLA were discussed in Section 2.2 (Freeze-Dried Systems) (Spinella and others 2015). Additionally, CNCs extracted with blends of acetic acid–HCl or butyric acid–HCl were shown to be redispersible in toluene (Braun and Dorgan 2009). Carboxylation is typically accomplished on CN surfaces via the use of TEMPO during extraction, predominately for CNFs. TEMPO is a relatively expensive chemical, and efforts have been undertaken to replace it. Tabar and others (2017) exposed never-dried wood pulp to an enzyme treatment followed by addition of syringic acid and ozone gas. After ultrasonification, the CNFs exhibited carboxylation levels similar to those from TEMPO oxidation. The syringic acid was proposed as an oxidation enhancer where it could be substituted for existing lignin in the biomass or pulp. An alternative approach to the same end is the use of molten oxalic acid for the hydrolysis and simultaneous carboxylation of biomass to CN (Li and others 2017). An added benefit of this approach is the ability to reuse the oxalic acid with separation taking place via its crystallization after cooling.

There is a large number of CN surface modification methods that rely on hazardous solvents and reactants as well as difficult to remove solvents. An example is that sulfuric-acid-extracted CNCs are dispersible in dimethyl sulfoxide, a solvent commonly used in its further surface modification. Its atmospheric pressure boiling point is 189 °C, making its removal difficult. This typically forces researchers to resort to high-*g* centrifugation to isolate the reaction products. Yoo and Youngblood (2016) developed a method for surface modification starting with the CNs in their as-extracted aqueous dispersion. They combined aqueous CNCs with an excess of DL-lactic acid in a round bottom flask and heated it to 180 °C in the presence of zinc acetate dehydrate catalyst. After approximately 80% of the water was removed, a fatty acid was added to the reaction vessel. Dibutyltin dilaurate was also added as a catalyst, and the reaction temperature was increased to 190 °C with vacuum applied to remove excess lactic acid. When the reaction was completed and cooled, the products were separated by low-*g* centrifugation with ethanol washing. The products were dried under vacuum at 50 °C for 24 h.

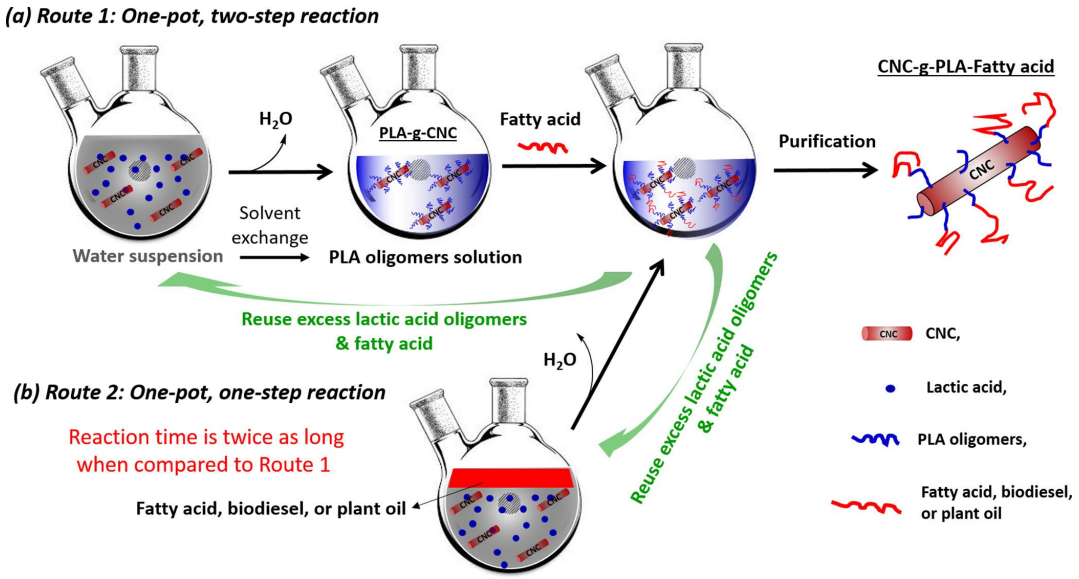

Figure 10—Reaction scheme for one-pot esterification of CNs via two different routes. (Reprinted with permission from Yoo and Youngblood (2016). Copyright 2016 American Chemical Society.)

Alternatively, the surface modification can be run by adding the fatty acid and tin catalyst to the aqueous CNC–lactic acid at the start of the reaction. Both methods are graphically shown in Figure 10. Thereby, the reaction can be completed in a single two-times-longer step. These methodologies present a process for taking aqueous CNCs and directly converting them to the hydrophobic state with control and specificity without time-consuming phase transfers or solvent removals. The authors noted that both the lactic acid removed under vacuum during the reaction and the unreacted fatty acid removed by centrifugation can be reconcentrated and reused. A variety of fatty acids were attached to the PLA-modified CNCs and were evaluated for their dispersibility in various solvents. It was found that dispersibility in hydrophobic solvents increased with fatty acid chain length and degree of substitution.

Hu and others (2017) developed a methodology with aims similar to Yoo and Youngblood (2016). The result is most likely the simplest and most direct routes to hydrophobic CN. Taking inspiration from mussel-dopamine-based adhesives, a high phenol content biomolecule was used to modify the surface of CNs as a first step toward facile hydrophobization and simultaneous isolation. Specifically, tannic acid was added to ultrasonically redispersed spray-dried CNCs in ambient temperature water at pH 8.0 and stirred for 6 h. Then decylamine was added, and the mixture was stirred for 3 h. The CNCs were transformed to the hydrophobic state via reaction between the bound tannic acid and the decylamine and were then spontaneously separated from the aqueous phase. The reaction scheme and images of the products are shown in Figure 11. The researcher's isolation method was by low-*g* centrifugation and washing with ethanol followed by freeze-drying or oven-drying. Both tannic acid and tannic acid–decylamine modified CNCs form liquid crystalline order in water and toluene, respectively. This indicates that CNCs are modified as individuals and retain their intraparticle coordination, which leads to long range order in the liquid state.

Next, we consider approaches to CN drying, surface modification, compatibilization, and incorporation in hydrophobic polymers. Drying is a major challenge for nanodispersions in water. How does one remove or replace the water while maintaining a redispersible nanomaterial or dispersion, respectively? Laaksonen and others (2017) took a different approach to water removal. They found that G-valerolactone and ionic liquids with anion proton affinities below 330 kcal/mol and Kamlet-Taft β values below 0.85 stabilized CNCs during dewatering such that hornification

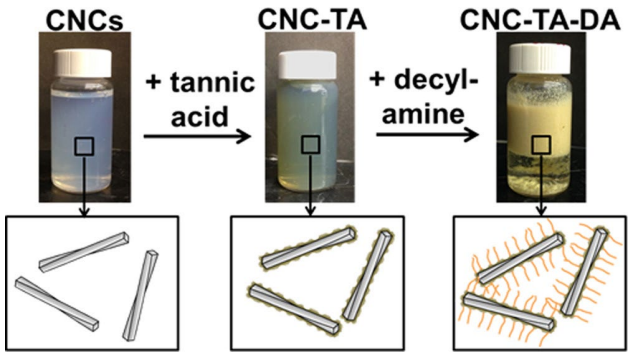

Figure 11—Reaction schematic of the treatment of aqueous CNCs with tannic acid followed by reaction with decylamine and phase separation from the aqueous phase. (Reprinted with permission from Hu and others (2017). Copyright 2017 American Chemical Society.)

was avoided and surface modification could be carried out in the absence of water. Asadi and others (2016) avoided the issue of drying by using as-produced CNs in the aqueous state in place of chemical sizing agents on glass fibers that required a post-application drying step. They briefly immersed glass fiber rovings in a CNC aqueous dispersion then dried the coated fibers in ambient conditions for 24 h. These were chopped and combined with an amine-cured epoxy, degassed, and cured at 60 °C for 1 h. The tensile properties were not significantly changed. However, the flexural modulus, strength, and elongation to failure were all improved substantially. Uribe and others (2017) dipped unsized carbon and glass 0/90° plain-weave fabrics into aqueous TEMPO-CNFs such that they achieved a 0.02 and 0.03 wt% gain, respectively, and then dried them for 3 h at 102 °C. These CNF-sized fabrics were used separately to create five-layer composites with quasi-isotropic stack sequence consisting of three aligned layers and two layers rotated 90° between sheets 1-3 and 3-5. This assembly was placed in a vacuum bag and infused with a two-component amine-cured epoxy and cured at ambient temperature for 24 h. Atomic force microscopy revealed that CNFs had deposited on the surface of the unsized fibers, resulting in a uniform coverage of the surface. Tensile properties did not increase by much. However, in agreement with Asadi and others (2016), flexural testing revealed notable increases in ultimate strength, modulus, and toughness, with the glass fiber responding more positively. In a similar manner, although a lower modulus fabric, jute fabric was coated with an aqueous dispersion of jute-derived CNF (Jabbar and others 2017). This was dried, coated with an amine–epoxy mixture, assembled into a multilayer composite, and cured under compression. As seems to be a common theme for such coated fiber composites, these composites did not exhibit a substantial increase in tensile properties. Instead, the flexural modulus and strength increased from the coating of the fibers with CNFs.

Looking to evaluate a straightforward industrial practice, Wang and others (2018) spray-dried (SD) an aqueous dispersion of CNFs in a pilot-scale spray drier at 250 °C. The spherical particles were blended with maleic anhydride functionalized PP (MAPP) and/or PP in a TSE. The SD CNF agglomerates maintained their spherical shape in the PP. The addition of MAPP appeared to decrease the larger agglomerates and improve dispersion. Both 30 wt% SD CNFs and 30/2 wt% SD CNF/MAPP composites exhibited significant improvements in tensile and flexural modulus at the expense of elongation with tensile modulus ratios of 1.9 and 2, respectively. Taking a similar approach, Gupta and others (2017) combined SD lignin-coated CNCs (SD L-CNCs) with 3D printing extrusion grade PLA (4043D) in a melt mixer. Here, the L-CNCs were extracted from biomass via a proprietary AVAP process and then coated with lignin (Nelson and Retsina 2014). Crystallinity of the PLA was increased by more than seven times at a 0.3 wt% loading accompanied by an approximately 17 °C drop in crystallization temperature. Storage modulus below T_g increased at 0.3 and 0.5 wt% L-CNCs reaching a modulus ratio of 1.7. This sharply dropped at 0.7 to 1 wt% and, at 2.5 wt%, recovered to values similar to those of 0.3 wt%. This trend follows the changes in percentage crystallinity indicating nucleation of PLA crystals at low CN and reinforcement with less crystallinity at higher CN loading. Above T_g, the higher crystallinity of the composites resulted in approximately two orders of magnitude increase in rubbery modulus (E_{RR} = 200). These results indicate possible improvement in heat deflection temperature, a known weakness of PLA. The researchers went on to attempt blown film processing of PLA and the composites. The PLA film bubble was unstable, whereas the composite film maintained the bubble shape, which facilitated film production. Wei and others (2018) conducted an evaluation of the same SD L-CNCs in a reactive extrusion grade PLA (4044D). They blended SD L-CNCs or high lignin CNCs (HL-CNC) with PLA in a lab-scale TSE with zones varying from 175 to 185 °C. Test specimens were injection-molded at 185 °C. The HL-CNCs were created by applying a sulfuric acid hydrolysis extraction procedure to heat-treated wood chips followed by freeze-drying to remove water. The differences between these lignin CNs are that the L-CNCs have considerably more hemicellulose and less lignin than the HL-CNCs. The composites exhibited increased modulus and elongation to break with a slight decrease in ultimate tensile strength regardless of CN type. The tensile modulus ratios ranged from 1.1 to 1.3 regardless of CN type. The HL-CNC additions increased the toughness measured as the area under the stress–strain curve. DMA testing revealed all composites improved the glassy modulus of PLA with the HL-CNCs doing this to a greater extent. However, none of the composites exhibited the large increase in crystallinity and the associated higher modulus above T_g observed by Gupta and others (2017). Perhaps this was caused by the difference in PLA grades or processing methods. Both grades contain the same D-PLA content, and the technical data sheets do not reveal obvious evidence for this difference.

Dewatering of CNs for composite applications is a step that presents a significant time and energy barrier for implementation. Here, approaches will be discussed that directly confront this issue, such as oven-drying, processing methods that only need partial dewatering, dewatering during preparation for composite blending, and dewatering during composite blending. Sato and others (2016) mixed filter-dewatered CMFs with N-methylpyrilidone, hexadecenylsuccinic anhydride, and a pyridine catalyst for 1 h at 70 to 80 °C. The still-wet modified CMFs were fed into a food mixer with maleic anhydride functionalized PP and high density polyethylene (HDPE). This blend was next put through a TSE at 98 °C and then again at 140 °C, followed by injection-molding of the resultant pellets at

160 °C. Composites with a 0.44 degree of substitution provided the largest increase in tensile modulus (E_R = 1.9) and ultimate tensile strength at the expense of elongation to failure. Miyazaki and others (2013) used a similar approach to dewatered CMFs and then added ethanol to fabricate a slurry that could be fed directly into a melt mixer along with syndiotactic PP (SPP). Volatization of the ethanol took place via low temperature mixing followed by melt-blending at 165 °C. Tensile testing revealed that the ethanol-swollen CMFs had a significantly increased modulus at 30 wt%, yielding a modulus ratio of 2.9, but had a substantial loss in elongation. The crystallinity of SPP was increased from 22% to 33%. Nechita and Panaitescu (2013) mechanically dewatered CMFs with carboxymethyl cellulose and then acetylated it. The functionalized CMFs were precipitated, washed, and oven-dried or spray-dried prior to blending with PP at ~175 °C. Both oven-dried and spray-dried CMFs increased modulus by 1.8 times at 10 wt% with the spray-dried increasing the modulus further to three times at 20 wt%. The use of acetylated CMFs at 5 wt% resulted in an E_R = 1.6 versus 1.2 for nonacetylated.

A plasticizer slurry approach was evaluated on CNCs blended with triethyl citrate and ethanol directly from the aqueous dispersed state (Herrera and others 2016). This formed a pumpable blend that was added directly to the mixing zone of a TSE along with PLA. The mixing zones in the extruder ranged from 170 °C at the addition point to 200 °C at the die with two off-gassing zones and a vacuum zone in between. The composites exhibited substantially improved yield strength and tensile modulus (E_R = 3.7) with all systems having high elongation to failure when the samples were rapidly cooled due to the presence of the plasticizer and low crystallinity. After slow cooling, the films lost transparency and the composites exhibited the more traditional gains in modulus (1.5 E_R) and tensile strength with a loss in elongation. Many similar studies used this slurry method. Effective modifications include precipitation of the aqueous CN–polymer solution followed by processing (E_R = 2.5) (Cao and others 2017), use of a CNC aqueous dispersion as the blowing agent in a urethane foam (compressive E_{C-R} = 1.6) (Cordero and others 2015), or blending CNC with a slurry containing a polymeric compatibilizer followed by melt-blending with the matrix after drying (E_R = 1.5) (Gray and others 2018).

Alternatively, water can be partially or fully removed directly by oven-drying. Generally, this is not a promising approach because it can lead to hornification. Yeo and others (2017) oven-dried CMFs, then silane-treated the powder in a glycidyloxypropyl triethoxysilane alcohol–water solution at pH 272. The CMFs were isolated by vacuum filtration and oven-dried once more. The resulting powder was added to an amine hardener–epoxy resin mixture and stirred for 10 min. Surprisingly, both modulus and tensile strength were notably increased compared with the unmodified CMF control and the unfilled matrix at loadings of 20 wt% (E_R = 2.7). It is important to note that in this silane approach, the products were washed with water and ethanol during vacuum filtration and dried at 50 °C. Based on the discussion of optimal silane modification of cellulose in Section 2.2, this approach may have washed some of the absorbed silanol oligomers away and then not fully condensed them by heating below 100 °C. Yet notable performance enhancements were gained. In a similar approach, a CMF water slurry was blended with poly(vinyl alcohol) (PVA) and HDPE pellets followed by oven-drying to 1 wt% moisture (Kiziltas and others 2016). This was then blended at 180 °C in an internal mixer, dried again in an oven, and injection-molded at 180 °C. The CNF–PVA composites displayed moderately increased tensile strength and modulus (E_R = 1.2) as well as flexural strength and modulus at the expense of impact strength.

There is great diversity in approaches that achieve surface functionalization or hydrophobic polymer incorporation without freeze-drying or solvents that are toxic or difficult to remove. The approaches summarized briefly in this section include extraction-based functionalization, one-pot surface modification of CN aqueous dispersions to the hydrophobic state, use of CNs as a beneficial fiber sizing treatment, industrial spray-drying, composite fabrication processes that use a slurry of CNs in water or ethanol with a plasticizer added in some situations to improve compatibility, and finally simple oven-drying. It is important to note that many of the surface modification methods discussed in this section have yet to be evaluated in composite applications. Thus, their full potential remains untested. Overall, these alternative methods offer industrial product developers many tools by which CNs can be directly evaluated in a wide range of products.

3. Conclusions

This review provides a summary of industrially applicable methods for the fabrication of CN-reinforced polymer matrix composites without the need for time-consuming or multistep procedures, toxic chemicals, or difficult to remove solvents. Beyond increases in modulus, which have been the focus of preceding discussions, CN reinforcement of polymer composites provides many additional benefits, such as enhancements in tensile and flexural strength, crystallinity, heat deflection temperature, coefficient of thermal expansion, crystallization rate, etc. Industrial products that are produced and applied in an aqueous medium, such as latices, allow for straightforward incorporation of WB CNs via the as-produced aqueous dispersion. Such applications are potentially the lowest barriers to entry for CNs into the industrial composites marketplace, with the WB adhesives, film converting, and coatings markets being of substantial scale and diversity. It has been demonstrated that freeze-drying CNs is an

effective means of obtaining water-free CNs that can be surface-modified or directly incorporated into hydrophobic polymers for performance enhancements. But the time-consuming nature of this method and the tendency to yield mildly to strongly agglomerated CNs render it suboptimal for composite production. Nonetheless, the methods applied to the FD CNs can potentially be combined with the alternative methods summarized in this review. The alternative methods do not depend on WB systems or FD CN. Therefore, they offer industrial product developers many tools by which CNs can be directly evaluated in a wide range of polymer composites and polymer-based products.

4. Knowledge Gaps

Following are the remaining challenges that must be overcome to advance both the manufacture and industrial use of cellulosic nanomaterials:

- Silane surface modification of cellulose is not as facile as with inorganic reinforcing materials. The ideal conditions for such chemistry to take place are aqueous hydrogen bonding of silanol oligomers to the surface of CNs followed by heating to more than 100 °C to cause condensation to a covalent bond. It seems unlikely that this second step would be efficient while the CN is in the aqueous state. However, washing of the CNs during water removal reportedly removes much of the hydrogen-bonded silanol. Thus, alternative methods need to be developed, indicating that the full potential of silane modification of CNs may not yet have been harnessed.
- Concentration of CNs without agglomeration via industrially viable means is a challenge that, once overcome, could greatly facilitate their use in WB applications.
- A rapid drying process that produces easily redispersible CNs is a challenge that, once solved, could greatly benefit nearly all CN endeavors. Perhaps this could take the form of improved spray-drying.
- Industrially scalable CN surface modifications that produce a surface that is reactive with the matrix is a need for producing optimally performing polymer–CN composites.
- CN optimal spacing between dispersed CNs or CN bundles appears to provide better performance enhancements. A fuller understanding of the mechanics of this enhanced reinforcement would be beneficial in recognizing its occurrence and facilitating its reproduction.
- CN killer applications, loosely defined as the meeting between an important market need and a key material property, character, etc., could garner the attention of industry and consumers.

5. Research Needs

Following are specific technical issues and challenges that, if solved, would have the greatest impact on closing the gap and lead to breakthroughs or new technology methods to advance the commercialization of cellulosic nanomaterials:

- No comparisons with industrial reinforcing phases were included in the reviewed literature. This may act as a significant barrier to industrial interest. Perhaps a bench marking study should be undertaken to create industrially relevant polymer composite products with CNs via methods discussed in this review or other suitable methods and compare them against similarly fabricated composites with currently used reinforcing phases.
- Because of the diversity in CN extraction processes and sources, it is vital that publications provide clear images of the CN in its final extracted and purified state prior to other treatments. The CNs should be diluted such that when deposited on a substrate for imaging, they are not stacked on top of each other or intertwined. This will allow for ease of identifying the type of CN and dimensions. This same procedure should be undertaken again after all processes and treatments have taken place and before incorporation into the composite, allowing changes in dimension to be accounted for.
- The state of CN dispersion in polymers is a vital aspect of its ability to provide reinforcement, particularly above T_g. Clear images of the state of dispersion in the polymer need to be provided in publications. The birefringent nature of CNs makes polarized optical microscopy ideal for evaluating the macro and micro state of dispersion in optically transparent composites. A DMA storage modulus above T_g appears to provide an indication of the state or effectiveness of the dispersion. Inclusion of these data would also be beneficial.
- Non-surface-modified CN–polymer composites show faster and, in some cases, greater moisture uptake. How does this impact product performance, and what can be done to control or mitigate it?
- Research should be carried out to determine how susceptible CN–polymer composites are to degradation from microorganisms (e.g., fungi and bacteria). Additionally, the impact of surface modification including hydrophobization and imparted reactive sites should also be evaluated.
- Solvents that are readily removed via industrially scalable processes need to be identified for use with CN surface modification.
- Methods or additives that assist in the disruption of CN self-affinity need to be investigated. Knowledge in this area would greatly facilitate the incorporation of CNs into WB polymer products such as coatings.
- Sedimentation of CNs during WB NR drying was frequently reported. Investigations should be carried out

to discern how widespread this issue is and what can be done to mitigate it.
- Research should be carried out to develop or discover compatibilizers that do not sacrifice stiffness.
- Many of the methods for surface modification discussed in this review have not been evaluated in polymer matrices, and many others have only been evaluated in one or two polymers. Research should be carried out to test the untried methods and benchmark the other methods with a wider variety of polymers–resins as appropriate with specific evaluations conducted to gauge viability in industrial conditions.

6. Acknowledgments

The authors acknowledge APPTI for their assistance in framing the scope and focus of this review. The authors acknowledge Dr. Kim Nelson of GranBio who provided assistance with screening the publications and many productive discussions. The authors acknowledge Prof. Meisha Shofner of the Georgia Institute of Technology for many productive discussions and reviewing the drafts and providing many helpful comments. The authors acknowledge Prof. Jeff Youngblood of Purdue University and Dr. Alan Rudie of the USDA Forest Service, Forest Products Laboratory for reviewing the drafts and providing many helpful comments.

7. Literature Cited

Abraham, E.; Elbi, P.A.; Deepa, B.; Jyotishkumar, P.; Pothen, L.A.; Narine, S.S.; Thomas, S. 2012. X-ray diffraction and biodegradation analysis of green composites of natural rubber/nanocellulose. Polymer Degradation and Stability. 97(11): 2378-2387. https://doi.org/10.1016/j.polymdegradstab.2012.07.028.

Amin, K.N.M.; Amiralian, N.; Annamalai, P.K.; Edwards, G.; Chaleat, C.; Martin, D.J. 2016. Scalable processing of thermoplastic polyurethane nanocomposites toughened with nanocellulose. Chemical Engineering Journal. 302: 406-416. https://doi.org/10.1016/j.cej.2016.05.067.

Annamalai, P.K.; Dagnon, K.L.; Monemian, S.; Foster, E.J.; Rowan, S.J.; Weder, C. 2014. Water-responsive mechanically adaptive nanocomposites based on styrene-butadiene rubber and cellulose nanocrystals-processing matters. ACS Applied Materials & Interfaces. 6(2): 967-976. https://doi.org/10.1021/am404382x.

Arias, A.; Heuzey, M.C.; Huneault, M.A.; Ausias, G.; Bendahou, A. 2015. Enhanced dispersion of cellulose nanocrystals in melt-processed polylactide-based nanocomposites. Cellulose. 22(1): 483-498. https://doi.org/10.1007/s10570-014-0476-z.

Asadi, A.; Miller, M.; Moon, R.J.; Kalaitzidou, K. 2016. Improving the interfacial and mechanical properties of short glass fiber/epoxy composites by coating the glass fibers with cellulose nanocrystals. Express Polymer Letters. 10(7): 587-597. https://doi.org/10.3144/expresspolymlett.2016.54.

Ben Elmabrouk, A.; Thielemans, W.; Dufresne, A.; Boufi, S. 2009. Preparation of poly(styrene-co-hexylacrylate)/cellulose whiskers nanocomposites via miniemulsion polymerization. Journal of Applied Polymer Science. 114(5): 2946-2955. https://doi.org/10.1002/app.30886.

Ben Mabrouk, A.; Kaddami, H.; Boufi, S.; Erchiqui, F.; Dufresne, A. 2012. Cellulosic nanoparticles from alfa fibers (*Stipa tenacissima*): extraction procedures and reinforcement potential in polymer nanocomposites. Cellulose. 19(3): 843-853. https://doi.org/10.1007/s10570-012-9662-z.

Bondeson, D.; Oksman, K. 2007. Dispersion and characteristics of surfactant modified cellulose whiskers nanocomposites. Composite Interfaces. 14(7-9): 617-630. https://doi.org/10.1163/156855407782106519.

Braun, B.; Dorgan, J.R. 2009. Single-step method for the isolation and surface functionalization of cellulosic nanowhiskers. Biomacromolecules. 10(2): 334-341. https://doi.org/10.1021/bm8011117.

Cao, X.D.; Xu, C.H.; Liu, Y.H.; Chen, Y.K. 2013a. Preparation and properties of carboxylated styrene-butadiene rubber/cellulose nanocrystals composites. Carbohydrate Polymers. 92(1): 69-76. https://doi.org/10.1016/j.carbpol.2012.09.054.

Cao, X.D.; Xu, C.H.; Wang, Y.P.; Liu, Y.; Liu, Y.H.; Chen, Y.K. 2013b. New nanocomposite materials reinforced with cellulose nanocrystals in nitrile rubber. Polymer Testing. 32(5): 819-826. https://doi.org/10.1016/j.polymertesting.2013.04.005.

Cao, L.M.; Fu, X.F.; Xu, C.H.; Yin, S.H.; Chen, Y.K. 2017. High-performance natural rubber nanocomposites with marine biomass (tunicate cellulose). Cellulose. 24(7): 2849-2860. https://doi.org/10.1007/s10570-017-1293-y.

Cataldi, A.; Berglund, L.; Deflorian, F.; Pegoretti, A. 2015. A comparison between micro- and nanocellulose-filled composite adhesives for oil paintings restoration. Nanocomposites. 1(4): 195-203. https://doi.org/10.1080/20550324.2015.1117239.

Chen, Y.K.; Zhang, Y.B.; Xu, C.H.; Cao, X.D. 2015. Cellulose nanocrystals reinforced foamed nitrile rubber nanocomposites. Carbohydrate Polymers. 130: 149-154. https://doi.org/10.1016/j.carbpol.2015.05.017.

Cordero, A.I.; Amalvy, J.I.; Fortunati, E.; Kenny, J.M.; Chiacchiarelli, L.M. 2015. The role of nanocrystalline cellulose on the microstructure of foamed castor-oil polyurethane nanocomposites. Carbohydrate Polymers. 134: 110-118. https://doi.org/10.1016/j.carbpol.2015.07.077.

CSA Group. 2014. CSA Z5100-14. Cellulosic nanomaterials — test methods for characterization. Toronto, Canada: CSA Group.

EPA. 2021. Toxic substances control act chemical substance inventory. Washington, DC: U.S. Environmental Protection Agency. https://www.epa.gov/tsca-inventory (accessed April 6, 2021).

Espinosa, S.C.; Kuhnt, T.; Foster, E.J.; Weder, C. 2013. Isolation of thermally stable cellulose nanocrystals by phosphoric acid hydrolysis. Biomacromolecules. 14(4): 1223-1230. https://doi.org/10.1021/bm400219u.

Farahbakhsh, N.; Roodposhti, P.S.; Ayoub, A.; Venditti, R.A.; Jur, J.S. 2015. Melt extrusion of polyethylene nanocomposites reinforced with nanofibrillated cellulose from cotton and wood sources. Journal of Applied Polymer Science. 132(17): 41857. https://doi.org/10.1002/app.41857.

Favier, V.; Canova, G.R.; Cavaille, J.Y.; Chanzy, H.; Dufresne, A.; Gauthier, C. 1995a. Nanocomposite materials from latex and cellulose whiskers. Polymers for Advanced Technologies. 6(5): 351-355. https://doi.org/10.1002/pat.1995.220060514.

Favier, V.; Chanzy, H.; Cavaille, J.Y. 1995b. Polymer nanocomposites reinforced by cellulose whiskers. Macromolecules. 28(18): 6365-6367. https://doi.org/10.1021/ma00122a053.

Favier, V.; Cavaille, J.Y.; Canova, G.R.; Shrivastava, S.C. 1997. Mechanical percolation in cellulose whisker nanocomposites. Polymer Engineering and Science. 37(10): 1732-1739. https://doi.org/10.1002/pen.11821.

FDA. 2016. Substances generally recognized as safe. Silver Spring, MD: Food and Drug Administration. federalregister.gov/documents/2016/08/17/2016-19164/substances-generally-recognized-as-safe. Vol. 81, FR 54959, 96 pp.

Fortunati, E.; Armentano, I.; Zhou, Q.; Iannoni, A.; Saino, E.; Visai, L.; Berglund, L.A.; Kenny, J.M. 2012. Multifunctional bionanocomposite films of poly(lactic acid), cellulose nanocrystals and silver nanoparticles. Carbohydrate Polymers. 87(2): 1596-1605. https://doi.org/10.1016/j.carbpol.2011.09.066.

Foster, E.J.; Moon, R.J.; Agarwal, U.P.; Bortner, M.J.; Bras, J.; Camarero-Espinosa, S.; Chan, K.J.; Clift, M.J.D.; Cranston, E.D.; Eichhorn, S.J.; et al. 2018. Current characterization methods for cellulose nanomaterials. Chemical Society Reviews. 47(8): 2609-2679. https://doi.org/10.1039/c6cs00895j.

Gandini, A.; Belgacem, M.N. 2005. Modified cellulose fibers as reinforcing fillers for macromolecular matrices. Macromolecular Symposia. 221: 257-270. https://doi.org/10.1002/masy.200550326.

Girouard, N.; Schueneman, G.T.; Shofner, M.L.; Meredith, J.C. 2015. Exploiting colloidal interfaces to increase dispersion, performance, and pot-life in cellulose nanocrystal/waterborne epoxy composites. Polymer. 68: 111-121. https://doi.org/10.1016/j.polymer.2015.05.009.

Gray, N.; Hamzeh, Y.; Kaboorani, A.; Abdulkhani, A. 2018. Influence of cellulose nanocrystal on strength and properties of low density polyethylene and thermoplastic starch composites. Industrial Crops and Products. 115: 298-305. https://doi.org/10.1016/j.indcrop.2018.02.017.

Gruneberger, F.; Kunniger, T.; Zimmermann, T.; Arnold, M. 2014. Nanofibrillated cellulose in wood coatings: mechanical properties of free composite films. Journal of Materials Science. 49(18): 6437-6448. https://doi.org/10.1007/s10853-014-8373-2.

Gupta, A.; Simmons, W.; Schueneman, G.T.; Hylton, D.; Mintz, E.A. 2017. Rheological and thermo-mechanical properties of poly(lactic acid)/lignin-coated cellulose nanocrystal composites. ACS Sustainable Chemistry & Engineering. 5(2): 1711-1720. https://doi.org/10.1021/acssuschemeng.6b02458.

Habibi, Y. 2014. Key advances in the chemical modification of nanocelluloses. Chemical Society Reviews. 43(5): 1519-1542. https://doi.org/10.1039/c3cs60204d.

Habibi, Y.; Lucia, L.A.; Rojas, O.J. 2010. Cellulose nanocrystals: chemistry, self-assembly, and applications. Chemical Reviews. 110(6): 3479-3500. https://doi.org/10.1021/cr900339w.

Herrera, N.; Salaberria, A.M.; Mathew, A.P.; Oksman, K. 2016. Plasticized polylactic acid nanocomposite films with cellulose and chitin nanocrystals prepared using extrusion and compression molding with two cooling rates: effects on mechanical, thermal and optical properties. Composites Part A: Applied Science and Manufacturing. 83: 89-97. https://doi.org/10.1016/j.compositesa.2015.05.024.

Herzog, R.O.; Jancke, W. 1920. Über den Physikalischen Aufbau einiger Hochmolekularer Organisher Verbindungen. Ber Dtsch Chem Ges. 53: 2162-2164. Scherrer, P. Bestimmung der Inneren Struktur and der Grösse von Kolloidteilchen mittels Röntgenstrahlen. In Kolloidchemie: ein Lehrbuch, 3rd ed.; Zsigmondy, R. Ed.; Spamer. https://doi.org/10.1002/cber.19200531019.

Hong, J.; Kim, D.S. 2013. Preparation and physical properties of polylactide/cellulose nanowhisker/nanoclay composites. Polymer Composites. 34(2): 293-298. https://doi.org/10.1002/pc.22413.

Hu, Z.; Berry, R.M.; Pelton, R.; Cranston, E.D. 2017. One-pot water-based hydrophobic surface modification of cellulose nanocrystals using plant polyphenols. ACS Sustainable Chemistry & Engineering. 5(6): 5018-5026. https://doi.org/10.1021/acssuschemeng.7b00415.

Inai, N.H.; Lewandowska, A.E.; Ghita, O.R.; Eichhorn, S.J. 2018. Interfaces in polyethylene oxide modified cellulose nanocrystal - polyethylene matrix composites. Composites Science and Technology. 154: 128-135. https://doi.org/10.1016/j.compscitech.2017.11.009.

Iwamoto, S.; Yamamoto, S.; Lee, S.H.; Endo, T. 2014. Solid-state shear pulverization as effective treatment for dispersing lignocellulose nanofibers in polypropylene composites. Cellulose. 21(3): 1573-1580. https://doi.org/10.1007/s10570-014-0195-5.

Iyer, K.A.; Schueneman, G.T.; Torkelson, J.M. 2015. Cellulose nanocrystal/polyolefin biocomposites prepared by solid-state shear pulverization: superior dispersion leading to synergistic property enhancements. Polymer. 56: 464-475. https://doi.org/10.1016/j.polymer.2014.11.017.

Jabbar, A.; Militky, J.; Wiener, J.; Kale, B.M.; Ali, U.; Rwawiire, S. 2017. Nanocellulose coated woven jute/green epoxy composites: characterization of mechanical and dynamic mechanical behavior. Composite Structures. 161: 340-349. https://doi.org/10.1016/j.compstruct.2016.11.062.

Jamshidian, M.; Tehrany, E.A.; Imran, M.; Jacquot, M.; Desobry, S. 2010. Poly-lactic acid: production, applications, nanocomposites, and release studies. Comprehensive Reviews in Food Science and Food Safety. 9(5): 552-571. https://doi.org/10.1111/j.1541-4337.2010.00126.x.

Kargarzadeh, H.; Ahmad, I.; Abdullah, I.; Dufresne, A.; Zainudin, S.Y.; Sheltami, R.M. 2012. Effects of hydrolysis conditions on the morphology, crystallinity, and thermal stability of cellulose nanocrystals extracted from kenaf bast fibers. Cellulose. 19(3): 855-866. https://doi.org/10.1007/s10570-012-9684-6.

Kargarzadeh, H.; Sheltami, R.M.; Ahmad, I.; Abdullah, I.; Dufresne, A. 2015. Cellulose nanocrystal reinforced liquid natural rubber toughened unsaturated polyester: Effects of filler content and surface treatment on its morphological, thermal, mechanical, and viscoelastic properties. Polymer. 71: 51-59. https://doi.org/10.1016/j.polymer.2015.06.045.

Khiari, R. 2017. Valorization of agricultural residues for cellulose nanofibrils production and their use in nanocomposite manufacturing. International Journal of Polymer Science. 2017: 6361245. https://doi.org/10.1155/2017/6361245.

Khoshkava, V.; Kamal, M.R. 2014. Effect of drying conditions on cellulose nanocrystal (CNC) agglomerate porosity and dispersibility in polymer nanocomposites. Powder Technology. 261: 288-298. https://doi.org/10.1016/j.powtec.2014.04.016.

Kiziltas, A.; Nazari, B.; Kiziltas, E.E.; Gardner, D.J.S.; Han, Y.; Rushing, T.S. 2016. Cellulose nanofiber-polyethylene nanocomposites modified by polyvinyl alcohol. Journal of Applied Polymer Science. 133(6). https://doi.org/10.1002/app.42933.

Laaksonen, T.; Helminen, J.K.J.; Lemetti, L.; Langbacka, J.; del Cerro, D.R.; Hummel, M.; Filpponen, I.; Rantamaki, A.H.; Kakko, T.; Kemell, M.L.; Wiedmer, S.K.; Heikkinen, S.; Kilpelainen, I.; King, A.W.T. 2017. WtF-nano: one-pot dewatering and water-free topochemical modification of nanocellulose in ionic liquids or γ-valerolactone. ChemSusChem. 10(24): 4879-4890. https://doi.org/10.1002/cssc.201701344.

Li, D.; Henschen, J.; Ek, M. 2017. Esterification and hydrolysis of cellulose using oxalic acid dihydrate in a solvent-free reaction suitable for preparation of surface-functionalised cellulose nanocrystals with high yield. Green Chemistry. 19(23): 5564-5567. https://doi.org/10.1039/c7gc02489d.

Li, J.J.; Song, Z.Q.; Li, D.G.; Shang, S.B.; Guo, Y. 2014. Cotton cellulose nanofiber-reinforced high density polyethylene composites prepared with two different pretreatment methods. Industrial Crops and Products. 59: 318-328. https://doi.org/10.1016/j.indcrop.2014.05.033.

Lu, J.; Askeland, P.; Drzal, L.T. 2008. Surface modification of microfibrillated cellulose for epoxy composite applications. Polymer. 49(5): 1285-1296. https://doi.org/10.1016/j.polymer.2008.01.028.

Maia, T.H.S.; Larocca, N.M.; Beatrice, C.A.G.; de Menezes, A.; Siqueira, G.D.; Pessana, L.A.; Dufresne, A.; Franca, M.P.; Lucas, A.D. 2017. Polyethylene cellulose nanofibrils nanocomposites. Carbohydrate Polymers. 173: 50-56. https://doi.org/10.1016/j.carbpol.2017.05.089.

MatWeb. 2019. NatureWorks® Ingeo™ 3051D Injection Grade PLA (discontinued **). Blacksburg, VA: MatWeb, LLC. https://www.matweb.com/search/DataSheet.aspx?MatGUID=022f6212e6e0415c9f740b3db3d1ae7e&ckck=1. (accessed April 16, 2019).

Miyazaki, K.; Hamadate, M.; Terano, M.; Nakatani, H. 2013. Syndiotactic polypropylene/microfibrous cellulose composites: effect of filler size on tensile properties. Journal of Applied Polymer Science. 128(1): 915-922. https://doi.org/10.1002/app.38284.

Moon, R.J.; Martini, A.; Nairn, J.; Simonsen, J.; Youngblood, J. 2011. Cellulose nanomaterials review: structure, properties and nanocomposites. Chemical Society Reviews. 40(7): 3941-3994. https://doi.org/10.1039/c0cs00108b.

Moon, R.J.; Schueneman, G.T.; Simonsen, J. 2016. Overview of cellulose nanomaterials, their capabilities and applications. JOM. 68(9): 2383-2394. https://doi.org/10.1007/s11837-016-2018-7.

NatureWorks. 2019. Ingeo™ biopolymer 4032D technical data sheet. Plymouth, MN: NatureWorks, LLC. https://www.natureworksllc.com/~/media/Technical_Resources/Technical_Data_Sheets/TechnicalDataSheet_4032D_films_pdf.pdf. (accessed April 16, 2019).

Nechita, P.; Panaitescu, D.M. 2013. Improving the dispersibility of cellulose microfibrillated structures in polymer matrix by controlling drying conditions and chemical surface modifications. Cellulose Chemistry and Technology. 47(9-10): 711-719.

Nechyporchuk, O.; Pignon, F.; Do Rego, A.M.B.; Belgacem, M.N. 2016. Influence of ionic interactions between nanofibrillated cellulose and latex on the ensuing composite properties. Composites Part B: Engineering. 85: 188-195. https://doi.org/10.1016/j.compositesb.2015.09.030.

Nelson, K.; Retsina, T. 2014. Innovative nanocellulose process breaks the cost barrier. Tappi Journal. 13(5): 19-23. https://doi.org/10.32964/TJ13.5.19.

Neto, W.P.F.; Mariano, M.; da Silva, I.S.V.; Silverio, H.A.; Putauxe, J.L.; Otaguro, H.; Pasquini, D.; Dufresne, A. 2016. Mechanical properties of natural rubber nanocomposites reinforced with high aspect ratio cellulose nanocrystals isolated from soy hulls. Carbohydrate Polymers. 153: 143-152. https://doi.org/10.1016/j.carbpol.2016.07.073.

Ranby, B.G. 1949. Aqueous colloidal solutions of cellulose micelles. Acta Chemica Scandinavica. 3(5): 649-650. https://doi.org/10.3891/acta.chem.scand.03-0649.

Ranby, B.G. 1951. Cellulose and muscle - the colloidal properties of cellulose micelles. Discussions of the Faraday Society. (11): 158-164. https://doi.org/10.1039/DF9511100158.

Ranby, B.G. 1952. The cellulose micelles. Tappi Journal. 35(2): 53-58.

Ranby, B.G.; Ribi, E. 1950. Über den feinbau der zellulose. Experientia. 6(1): 12-14. https://doi.org/10.1007/bf02154044.

Raquez, J.M.; Murena, Y.; Goffin, A.L.; Habibi, Y.; Ruelle, B.; DeBuyl, F.; Dubois, P. 2012. Surface-modification of cellulose nanowhiskers and their use as nanoreinforcers into polylactide: a sustainably-integrated approach. Composites Science and Technology. 72(5): 544-549. https://doi.org/10.1016/j.compscitech.2011.11.017.

Reiner, R.S.; Rudie, A.W. 2013a. Pilot plant scale-up of TEMPO-pretreated cellulose nanofibrils. In: Postek, M.T.; Moon, R.J.; Rudie, A.W.; Bilodeau, M.A., eds. Production and Applications of Cellulose Nanomaterials. Peachtree Corners, GA: TAPPI Press: 177-178.

Reiner, R.S.; Rudie, A.W. 2013b. Process scale-up of cellulose nanocrystal production to 25 kg per batch at the Forest Products Laboratory. In: Postek, M.T.; Moon, R.J.; Rudie, A.W.; Bilodeau, M.A., eds. Production and Applications of Cellulose Nanomaterials. Peachtree Corners, GA: TAPPI Press: 21-24.

Ruiz, M.M.; Cavaille, J.Y.; Dufresne, A.; Gerard, J.F.; Graillat, C. 2000. Processing and characterization of new thermoset nanocomposites based on cellulose whiskers. Composite Interfaces. 7(2): 117-131. https://doi.org/10.1163/156855400300184271.

Saba, N.; Mohammad, F.; Pervaiz, M.; Jawaid, M.; Alothman, O.Y.; Sain, M. 2017. Mechanical, morphological and structural properties of cellulose nanofibers reinforced epoxy composites. International Journal of Biological Macromolecules. 97: 190-200. https://doi.org/10.1016/j.ijbiomac.2017.01.029.

Sanches, A.O.; Ricco, L.H.S.; Malmonge, L.F.; da Silva, M.J.; Sakamoto, W.K.; Malmonge, J.A. 2014. Influence of cellulose nanofibrils on soft and hard segments of polyurethane/cellulose nanocomposites and effect of humidity on their mechanical properties. Polymer Testing. 40: 99-105. https://doi.org/10.1016/j.polymertesting.2014.08.013.

Sato, A.; Kabusaki, D.; Okumura, H.; Nakatani, T.; Nakatsubo, F.; Yano, H. 2016. Surface modification of cellulose nanofibers with alkenyl succinic anhydride for high-density polyethylene reinforcement. Composites Part A: Applied Science and Manufacturing. 83: 72-79. https://doi.org/10.1016/j.compositesa.2015.11.009.

Spinella, S.; Lo Re, G.; Liu, B.; Dorgan, J.; Habibi, Y.; Leclere, P.; Raquez, J.M.; Dubois, P.; Gross, R.A. 2015. Polylactide/cellulose nanocrystal nanocomposites: efficient routes for nanofiber modification and effects of nanofiber chemistry on PLA reinforcement. Polymer. 65: 9-17. https://doi.org/10.1016/j.polymer.2015.02.048.

Tabar, I.B.; Zhang, X.M.; Youngblood, J.P.; Mosier, N.S. 2017. Production of cellulose nanofibers using phenolic enhanced surface oxidation. Carbohydrate Polymers. 174: 120-127. https://doi.org/10.1016/j.carbpol.2017.06.058.

Thomas, M.G.; Abraham, E.; Jyotishkumar, P.; Maria, H.J.; Pothen, L.A.; Thomas, S. 2015. Nanocelluloses from jute fibers and their nanocomposites with natural rubber: preparation and characterization. International Journal of Biological Macromolecules. 81: 768-777. https://doi.org/10.1016/j.ijbiomac.2015.08.053.

Uribe, B.E.B.; Chiromito, E.M.S.; Carvalho, A.J.F.; Arenal, R.; Tarpani, J.R. 2017. TEMPO-oxidized cellulose nanofibers as interfacial strengthener in continuous-fiber reinforced polymer composites. Materials & Design. 133: 340-348. https://doi.org/10.1016/j.matdes.2017.08.004.

Valadez-Gonzalez, A.; Cervantes-Uc, J.M.; Olayo, R.; Herrera-Franco, P.J. 1999. Chemical modification of henequen fibers with an organosilane coupling agent. Composites Part B: Engineering. 30(3): 321-331. https://doi.org/10.1016/s1359-8368(98)00055-9.

Wang, L.; Roach, A.W.; Gardner, D.J.; Han, Y. 2018. Mechanisms contributing to mechanical property changes in composites of polypropylene reinforced with spray-dried cellulose nanofibrils. Cellulose. 25(1): 439-448. https://doi.org/10.1007/s10570-017-1556-7.

Wei, L.Q.; Agarwal, U.P.; Matuana, L.; Sabo, R.C.; Stark, N.M. 2018. Performance of high lignin content cellulose nanocrystals in poly(lactic acid). Polymer. 135: 305-313. https://doi.org/10.1016/j.polymer.2017.12.039.

Yeo, J.S.; Kim, O.Y.; Hwang, S.H. 2017. The effect of chemical surface treatment on the fracture toughness of microfibrillated cellulose reinforced epoxy composites. Journal of Industrial and Engineering Chemistry. 45: 301-306. https://doi.org/10.1016/j.jiec.2016.09.039.

Yoo, Y.M.; Youngblood, J.P. 2016. Green one-pot synthesis of surface hydrophobized cellulose nanocrystals in aqueous medium. ACS Sustainable Chemistry & Engineering. 4(7): 3927-3938. https://doi.org/10.1021/acssuschemeng.6b00781.

Yu, H.Y.; Qin, Z.Y.; Liang, B.L.; Liu, N.; Zhou, Z.; Chen, L. 2013. Facile extraction of thermally stable cellulose nanocrystals with a high yield of 93% through hydrochloric acid hydrolysis under hydrothermal conditions. Journal of Materials Chemistry A. 1(12): 3938-3944. https://doi.org/10.1039/c3ta01150j.

Yue, L.; Maiorana, A.; Khelifa, F.; Patel, A.; Raquez, J.M.; Bonnaud, L.; Gross, R.; Dubois, P.; Manas-Zloczower, I. 2018. Surface-modified cellulose nanocrystals for biobased epoxy nanocomposites. Polymer. 134: 155-162. https://doi.org/10.1016/j.polymer.2017.11.051.

Zhang, C.M.; Dan, Y.; Peng, J.; Turng, L.S.; Sabo, R.; Clemons, C. 2014. Thermal and mechanical properties of natural rubber composites reinforced with cellulose nanocrystals from Southern Pine. Advances in Polymer Technology. 33 (S1): 21448. https://doi.org/10.1002/adv.21448.